Ecsel-2019-1-876190

Moore4Medical

"Accelerating Innovation in Microfabricated Medical Devices"

Deliverable D4.3:
Low frequency CMUT & PMUT demonstration report

Due date of deliverable: (01-10-2022)
Actual submission date: (18-10-2022)

Start date of Project: 01 June 2020   Duration: 36 months

Responsible WP4: Philips

Revision: final

	Dissemination level		
PU	Public		✔
PP	Restricted to other programme participants (including the Commission Service		
RE	Restricted to a group specified by the consortium (including the Commission Services)		
CO	Confidential, only for members of the consortium (excluding the Commission Services)		

Moore4Medical

Enabling "Moore for Medical"

0 DOCUMENT INFO

Authors

Editor Address data	Name: Rob van Schaijk Partner: Philips MEMS & Micro Devices Address: High Tech Campus 4, 5656 AE Eindhoven, The Netherlands E-mail: rob.van.schaijk@philips.com Fax: N/A
	Name: Alessandro Stuart Savoia Partner: Roma Tre University Address: Via della Vasca Navale 84, 00146 Rome, Italy E-mail: alessandro.savoia@uniroma3.it Fax: N/A
	Name: Fabio Quaglia Partner: ST Microelectronics Address: E-mail: fabio.quaglia@st.com Fax: N/A

Key words: micro fabrication, PMUT, CMUT, low frequency MUT, benchmark PMUT-CMUT

Documents history

Document version #	Date	Change
V0.1	05-07-22	Starting version, template
Sign off	28-09-22	Signed off version (for approval to PMT members)
V1.0	18-10-22	Approved Version to be submitted to ECSEL office

Distribution list

Date	Issue	E-mailer
		Huascar.Espinoza@kdt-ju.europa.eu
		Al_moore4medical@natlab.research.philips.com

Table of content

1 Executive summary

This report is a deliverable of the EU project Moore4Medical. Moore4Medical will accelerate innovation in electronic medical devices. The project addresses emerging applications and technologies that offer exciting new opportunities for the Electronic Components and Systems (ECS) industry. Moore4Medical will focus on the development of open and enabling technology platforms.

The WP4 topic is the development of next generation ultrasound. As part of this work package CMUT and PMUT technology platform will be developed to the level that they are suitable for on-body (low-frequency) imaging applications with both 1D (2D imaging) and 2D matrices (3D imaging). This implies the development of CMUT and PMUT microfabrication, new 3D integration schemes and front-end ASICs. This report describes the first results: PMUT and CMUT development for low frequency applications. This includes the development and optimization of CMUT and PMUT 1D arrays, acoustic module, and packaging. The performance of both technologies was tested extensively. Both were benchmarked with measurements performed at different sites.

The main contributors in this task are ST Microelectronics and Roma Tre University for PMUT and Philips for CMUT. For both technologies good acoustic performance was obtained, and first imaging results were promising. The benchmark between both technologies showed similar results measured at both sites. The CMUT has better receive sensitivity and larger bandwidth and PMUT better transmit sensitivity and lower harmonic distortion.

In the remainder of the project the PMUT and CMUT technologies will be used for 2D arrays integrated with ASIC for transmit and receive.

Moore4Medical

Enabling "Moore for Medical"

WP4 D4.3, version 1.0
Moore4Medical
Ecsel-2019-1-876190
Page 6 of 44

2 Introduction

This document describes the results that are the output of Task 4.2 of the Moore4Medical project. The goal of this task is to develop and test low-frequency ultrasound transducers that are realized using innovative micromachining techniques, intended for medical imaging. Capacitive micromachined ultrasound transducers (CMUTs) were realized by Philips, and piezoelectric micromachined ultrasound transducers (PMUTs) by ST-I. Testing of both transducer types was performed at Philips as well as Roma Tre University.

In the next sections we will provide background on medical ultrasound, followed by brief introductions of the cMUT and pMUT technologies.

2.1 Medical ultrasound transducers

Today's ultrasonic transducers for medical imaging are dominantly based on poly- or single-crystalline piezoelectric ceramics and composites. These piezoelectric materials became the reference for medical imaging because of their high piezoelectric constant and high electromechanical coupling coefficient. Piezoelectric ceramics require high-precision mechanical dicing into individual transducer elements making it expensive, especially for the fabrication of 2D arrays for 3D imaging in large consumer-size volumes and manufacturing of highly miniaturized and high-frequency transducers for use in intra cardiac echocardiography (ICE) and intravascular ultrasound (IVUS) catheters. On the other hand, micromachined ultrasonic transducers (MUTs) can be manufactured using standard microfabrication technologies thus significantly reducing the costly assembly steps needed for conventional piezoelectric and enabling miniaturization and high-frequency broadband operation.

The medical ultrasound application field for ultrasonic transducers is vast. It covers low frequency ultrasound (<3 MHz) for diagnostics and ablation, medium frequency ultrasound (3-10 MHz) for shallow on-body diagnostics and trans esophageal echocardiography (TEE), and high frequency (>10 MHz) for in-body coronary applications such as ICE and IVUS (see Table 1 [1]).

Table 1: Examples of ultrasonic transducers used for diagnostic and interventional imaging, and therapy.

Low frequency			Medium frequency			High frequency	
Echocardio-graphy	Abdominal	Therapeutic	Gynaecology	TEE	Vascular	ICE	IVUS
1-5 MHz	2-5 MHz	4-8 MHz	5-10 MHz	5-10 MHz	5-15 MHz	5-20 MHz	20-50 MHz

In the context of medical ultrasound applications, MEMS ultrasonic transducers are particularly attractive as they allow for on-body and in-body radiation-free operation together with low production cost, making them potentially appropriate for consumer-size markets. To summarize, the main advantages of MEMS ultrasonic transducers are:
- High volume production
- Eliminate (manual) assembly

Moore4Medical

Enabling "Moore for Medical"

WP4 D4.3, version 1.0
Moore4Medical
Ecsel-2019-1-876190
Page 7 of 44

- Low-cost platform → multiple applications (including consumer market)
- Miniaturization → catheters
- Higher frequencies
- 3D imaging compatible
- Easier coupling to body

This report focusses on low frequency ultrasound with centre frequency around 3MHz. The foreseen application fields for low frequency MEMS devices will be point of care applications with portable hand-held general-purpose probes and soon monitoring with patches. There are already many hand-held solutions on the market and an overview is shown in Figure 1. Most of those handheld probes are used for multiple imaging purposes in the low frequency range (2-8MHz), often with different probes for different applications. In this overview the column 'screen' indicates the image quality of the handheld probes.

MACHINE	PORTABILITY	BATTERY LIFE	PROBES	SCREEN	COST £	OVERALL SCORE
Sonon	++	++	3	++	14000	5
Vscan	++++	+++	2	+++	6000	9
Clarius	++	++	3	++	12000	4.5
iViz	+++	++	4	++++	19450	8.5
Butterfly	+++++	++++	1	+++	1600	8
Lumify	+++	+++	3	+++++	17000	8.5

Figure 1: comparison of different suppliers of hand-held probes [1].

All, except Butterfly, still rely on piezoelectric ceramics. Butterfly uses CMUT on ASIC for their hand-held probes [3]. Their main selling point is the ease of use with the help of artificial intelligence on the cloud. Another MEMS example is from EXO [2], which uses PMUT for a 3D imager with 4096 PMUT pixels. As soon as handheld probes are used more often, MUT will gain momentum due to their lower cost and platform use.

Moore4Medical

Enabling "Moore for Medical"
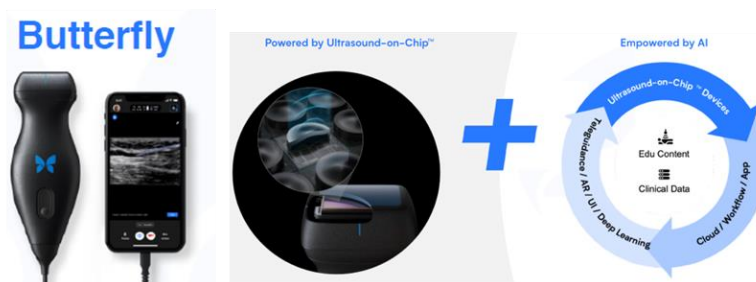
PMUT:

CMUT:

Figure 2: Examples of ultrasound probes on the market with PMUT and CMUT

2.2 Introduction to MUT technologies

A MUT consists of a thin membrane suspended above a cavity. There are two main types of MUTs, which differ in the transduction mechanism: capacitive micromachined ultrasonic transducers (CMUTs) are based on the electrostatic effect, while piezoelectric micromachined ultrasonic transducers (PMUTs) rely on the piezoelectric effect, see Figure 3 [4].

While traditional piezoelectric transducers are based on the thickness-mode vibration of bulk piezoelectric material or composite, MUT membranes vibrate in flexural mode, resulting in a much lower mechanical impedance. As a result, MUTs are intrinsically better acoustically matched to biological tissue and do not require the use of matching layers typically employed in traditional transducers to achieve broadband operation.

Figure 3: Ultrasound transducer technologies

2.2.1 CMUT

In a CMUT the vibrating membrane includes a conductive layer, which may be a metallic layer or a doped silicon layer. A conductive substrate acts as the bottom electrode. When a DC voltage is applied over these two electrodes, an electric field is generated inside the cavity, so that the top plate is attracted towards the substrate by an electrostatic force. Drivi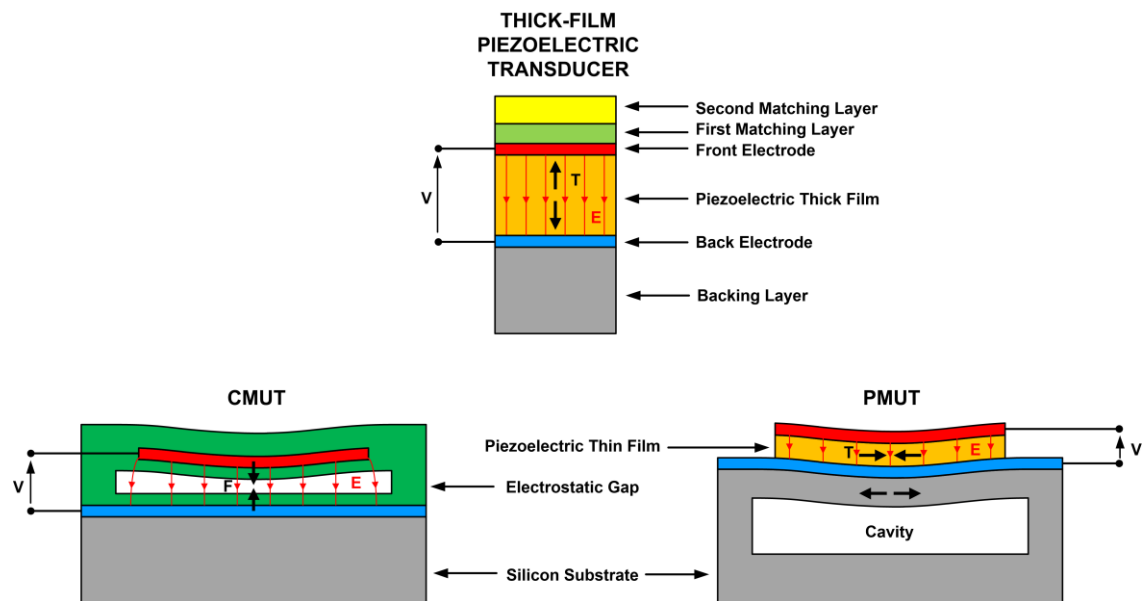ng the CMUT with an AC voltage sets the membrane into vibration and acoustic waves are generated in the surrounding medium. This mechanism also works oppositely. An acoustic wave causing the membrane to vibrate results in a capacitance variation, which is then converted in a variable voltage and/or current under electrical biasing of the CMUT. Efficient and stable electro-mechanical transduction requires generating and maintaining high electric fields in the gap. The key point to generating high acoustic pressures is to maintain large electric fields in the gap. The operating frequency is determined by the dimensions, shape and mechanical properties of the membrane. In collapse mode CMUTs, the cells are designed such that part of the (electrically isolated) membrane is in physical contact with the substrate during normal operation. The differences between collapsed and non-collapsed CMUT are schematically shown in Figure 4. The CMUT always operates with a DC voltage for good performance. For the non-collapse one the DC voltage should be significantly lower than the collapse voltage and vice versa for the collapsed version.
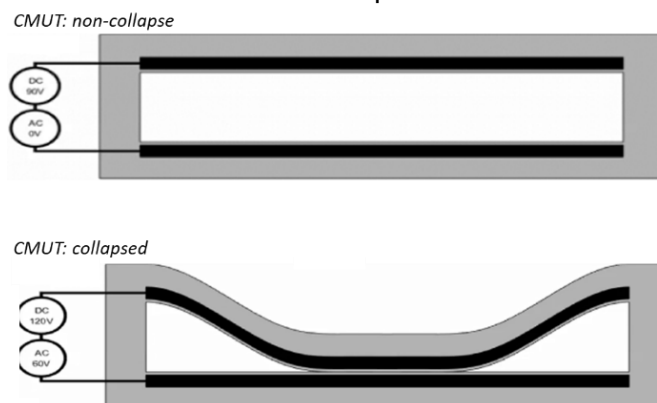
Figure 4: top: non-collapsed version CMUT with DC voltage is lower than collapse voltage. Bottom: collapsed version CMUT with DC voltage higher than collapse voltage.

Moore4Medical

Enabling "Moore for Medical"

WP4 D4.3, version 1.0
Moore4Medical
Ecsel-2019-1-876190
Page 10 of 44

2.2.2 PMUT

In a PMUT, the vibrating element consists of a multi-layer structure comprising a piezoelectric thin-film layer metalized on both sides and coupled to an elastic membrane suspended over a cavity. Typically, this structure covers part of the membrane. If an AC voltage is applied across the electrodes, an electrical field is generated in the thin-film piezoelectric layer, typically AlN or PZT, which results in stress in the membrane due to the piezoelectric effect. This stress relaxes into a vertical movement of the clamped membrane and thereby generates acoustic waves in the surrounding medium. Vice versa, the piezoelectric effect can also be used to detect acoustic waves impinging on the membrane. In general, a PMUT does not require a DC voltage to operate. However, if the piezoelectric material is ferroelectric, as PZT is, a DC voltage is applied to operate the PMUT in the linear regime, i.e., far from the coercive field.

3 Low frequency CMUT development

The low frequency CMUT is part of the CMUT platform from Philips [5][6] and the low frequency CMUT was developed during earlier EU projects [7][8]. During the Moore4Medical project, the low frequency CMUT technology was further developed and matured to be ready for product development, both for partners within and outside Philips. The main topics worked on in Task 4.2 were:

- Transfer from 150mm towards 200mm wafer size
- Process sensitivity investigated and effect on performance confirmed with corner batches
- Improvements of the acoustic CMUT module
- Development of low voltage CMUT variants

These topics are discussed in the following sections.

3.1 Low frequency CMUT transducer

3.1.1 Introduction

Capacitive micro-machined ultrasonic transducers (CMUTs) are MEMS based structures that transmit and receive acoustic signals in the ultrasonic range. They enable breakthrough applications for ultrasound, complementing conventional piezo technology with advantages such as small form factor, large bandwidth, easy fabrication of large arrays, and integration with driver circuitry: CMUT-on-CMOS for 3D ultrasound. The combination of processing CMUT devices with flexible foils [9] results in easier and cheaper integration in e.g., catheters. Our CMUT devices use the so-called collapse mode, with increased output pressure and sensitivity compared to devices in non-collapse mode. This technology is well suited and optimized for medical applications, ranging from general probes towards integration in catheters. For the first applications, it leverages the main CMUT advantages of high-volume manufacturing, low cost and high performance leading towards ubiquitous ultrasound. For the catheter-based devices, CMUT technology also adds high levels of integration and miniaturization.

3.1.2 Process flow CMUT

CMUT process flow is tailor-made for volume processing and is simple and robust. The CMUT processing is done on a single wafer (no wafer bonding), with only six masks needed. Full processing is done at low temperatures (<400°C), which makes easy integration with driver circuitry possible (CMUT-on-CMOS). Only common IC compatible materials are used for CMUT, meaning silicon oxide, silicon nitride and aluminium alloys. This CMUT technology can be tailored for different applications by tuning, drum design and layer stack. The centre frequency ranges from 1MHz up to 50MHz. The CMUT drum dimensions can vary from 20µm up to 400µm depending on the required centre frequency. Typical examples of current baseline processes are the low frequency variant (CM5), the drum size is 350µm (pitch 315µm) and for the medium frequency (CM12) it is 120µm (pitch 200µm). The vacuum gap height and membrane thickness are the main parameters in the layer stack to be tuned for the different CMUT variants. In general, for CMUT lower gap heights and thinner membranes results in higher frequencies.

Schematic process flow is shown in Figure 5:

Moore4Medical

Enabling "Moore for Medical"

A: Start material is silicon wafer with dielectric layer (oxide). Start material could also be an ASIC wafer with integrated electronics. On top of the oxide the bottom electrode (aluminium alloy) is deposited and patterned (mask 1).

B: On top of bottom electrode the first dielectric (SiO_2) is deposited. Next step is the deposition and patterning of the sacrificial metal (mask 2). This layer will be etched away later and forms the vacuum gap of the CMUT drum.

C: The second dielectric layer (SiO_2) is deposited and is the same as the first dielectric. On top of this layer the top electrode is deposited and patterned (mask 3).

D: The first part of the CMUT membrane (Si_3N_4) is deposited.

E: On the side of the drums an etch hole is patterned (mask 4). Through this hole the sacrificial material is removed, and the cavity is formed.

F: The etch hole is sealed by deposition of the second part of the membrane (Si_3N_4). This deposition is done in a low pressure forming the 'vacuum' gap. This Si_3N_4 seal goes partly inside the cavity, as shown in SEM picture (G). This is no issues, as the etch hole is located at a tab outside the active area of the CMUT device. The processing of CMUT is finished with etching vias (mask 5) and patterning of bond pads (mask 6) for contacting top and bottom electrodes.

G: SEM picture of part of CMUT membrane with sealed etch hole. In this case the CMUT is processed on top of ASIC wafer.
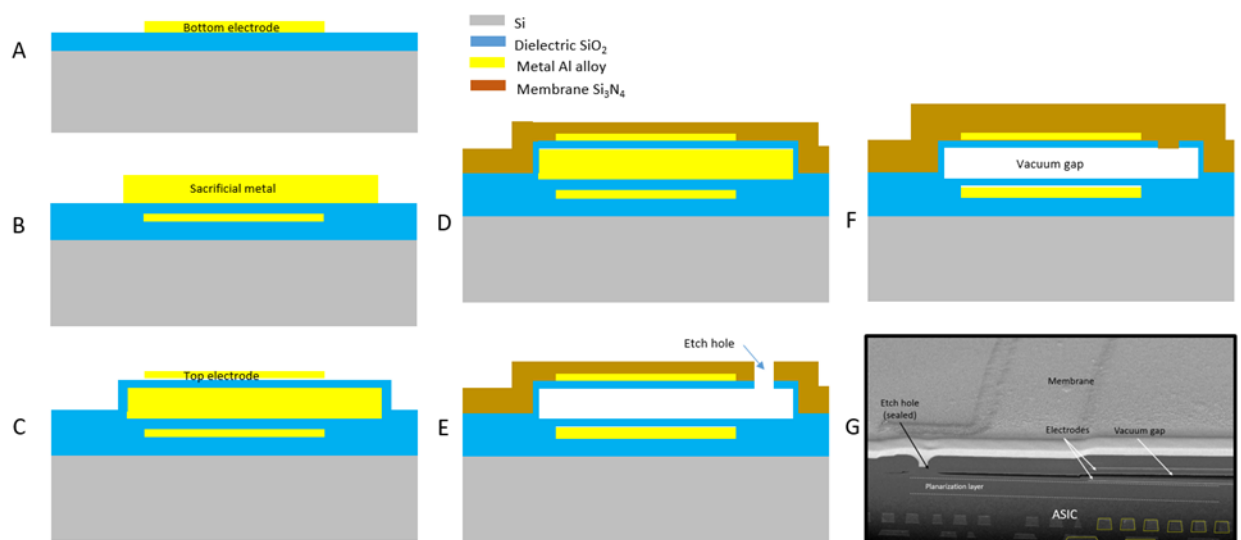
Figure 5: Schematic process flow low frequency CMUT

3.1.3 Comparison with Butterfly technology

The portable handheld product of Butterfly is currently the CMUT standard on the market. The characteristics of their technology can be analysed by studying reverse engineering report [11] and patents:

- 3 wafers for processing:
    - 2 SOI wafers for CMUT → wafer bonding needed to form cavity
    - 1 wafer for ASIC
        - CMUT wafers combined via wafer/die bonding
        - Additional Interposer
    - Interconnect between ASIC and CMUT with TSV
    - 300mm wafer size (assumption)
- 17 mask layer CMUT process
- Complex PCB used

Moore4Medical

Enabling "Moore for Medical"

— Very thin die
— Thick ceramic layer used → used as heat sink

Acoustic stack is a glass particles filled silicone rubber
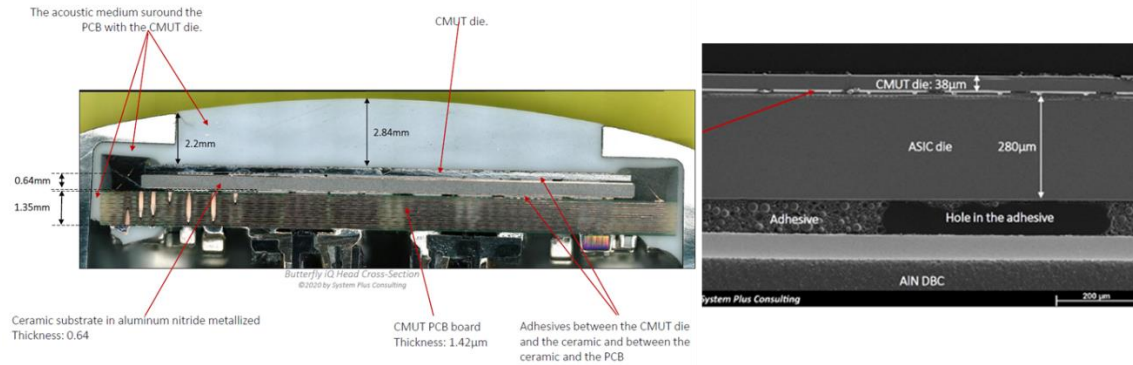
Figure 6: Cross-section of Butterfly probe [11]

At Philips, we believe that we have a simpler and more robust process flow for our CMUT technology. The main characteristics are:

- Single wafer
- Only 6 masks
- High packing density
- Low temperature → easy integration on top of ASIC wafer
- Standard processing and materials, like aluminum, silicon nitride and silicon oxide
- Lead free

The main differences are in the number of masks needed and the fact that no SOI or wafer bonding is used. To our opinion this makes the process flow easier and more robust.

3.1.4 Low frequency CMUT specifications

In Figure 7, the die with an active area of 12x21mm^2 and picture of part of the array are shown. The CM5 is a 1D phased array, suitable for beam steering as shown schematically in Figure 7. For our current CM5 process, we analyse the performance on wafer level. Also, we have an assembly process running that allows for measuring acoustical parameters. Furthermore, we have designed a lens stack that also allows for making images with the CM5 die.

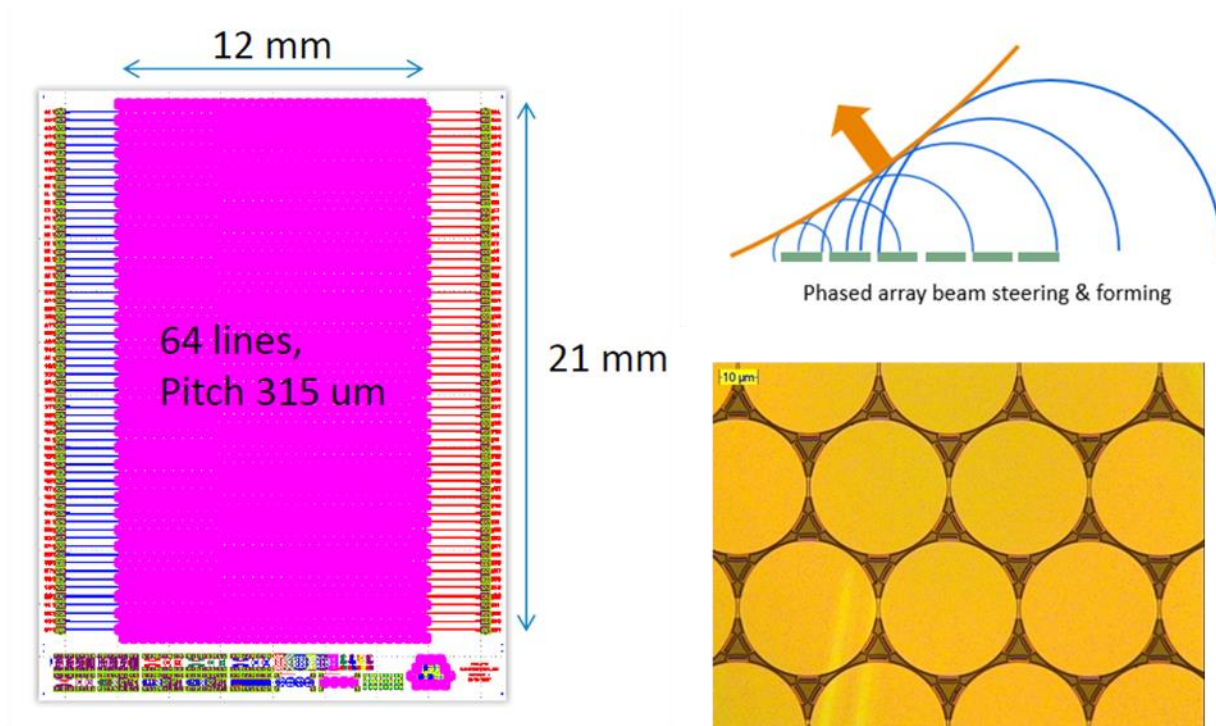*Figure 7: Sensor die with active area 12x21mm² (left), CMUT is phased array (top right) and part of sensor array with drums with 350µm diameter (bottom right)*

In the following Table 2, typical results of these evaluations are shown, as well as minimum and maximum values that we currently use. For each custom CMUT design, the specs for these parameters need to be developed and agreed upon.

Table 2: Typical values for the performance of low frequency CMUT (CM5) devices

Parameter	Min	Typ	Max	Unit	Notes
Wafer level					
Collapse voltage	30	50	70	V	1
Max. Voltage (Bias + RF)			170	V	2
Impedance: $F_{resonance}$	2.7	3.5	4.3	MHz	3
Impedance: coupling factor k_t^2	0.19	0.27	0.35	-	4
Impedance: capacitance (C_m + C_e)	160	225	290	pF	5
Drift			10	V	6
Acoustical characterization					
Centre frequency	2.4	3.0	3.6	MHz	7
Bandwidth (-3dB)	70	100	130	%	7
Maximum sound pressure	0.7	1.0	1.3	MPa	8
Sensitivity	1.7	2.0	2.3	MPa/100V RF	8
Frequency @ max. pressure		3.0		MHz	8
Voltage @ max. pressure		170		V	8
Imaging					
Penetration depth	20			cm	9
Resolution		750		µm	9
Lifetime, # pulses		1E10		-	9

Dimensions array		
Length	21	mm
Width	12	mm
Thickness	0.3-0.7	mm

Note 1: Collapse voltages (V_c) are determined with a fast linear DC bias sweep (-120V → 120V → -120V) with small RF voltage (1V; ~80MHz) superimposed, resulting in a standing wave where the phase depends on the impedance variation of the CMUT. Fast V_c measurements are standardly measured on all elements of all CM5 arrays on all wafers processed. This will result in a wafer map of the collapse voltage and give an indication of the number of functional elements. A typical curve is shown in Figure 8, showing the collapse and snap-back voltage for both positive and negative polarity. The V_c is an important parameter for process monitoring because it strongly depends on process quality and process variation.
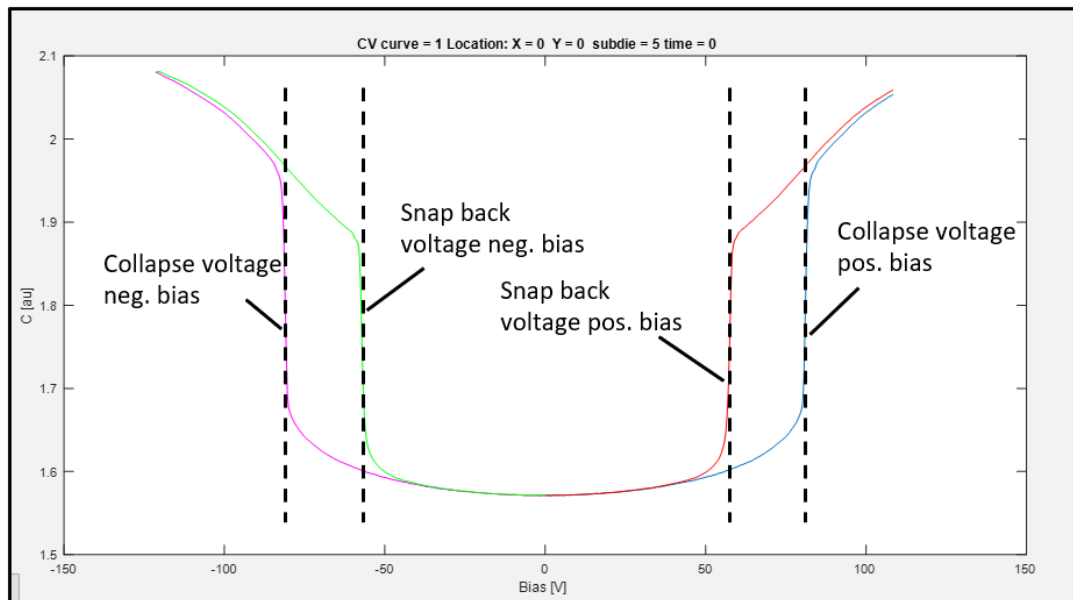

Figure 8: Typical example of 'impedance' measurement for determining collapse voltage.

Note 2: Maximum operational voltage is defined as sum of bias voltage + RF voltage. Suggested maximum operational voltage: bias 120V + 50V RF
Note 3: From impedance measurements (phase), the resonance frequency in air can be derived @ 120V bias (collapse mode). This frequency relates to centre frequency in immersion.
Note 4: From impedance measurements (magnitude), the coupling can be derived @ 120V bias. The coupling defines the amount of stored mechanical energy per input of electrical energy: $\frac{k_t^2}{(1-k_t^2)} = \frac{f_a^2 - f_r^2}{f_r^2}$, with f_a is anti-resonance frequency and f_r resonance frequency in (imaginary) part of impedance signal.
Note 5: Total capacitance ($C_m + C_e$) derived from impedance measurement @120 V bias (value derived from fit at high frequency)
Note 6: Maximum drift of collapse voltage during stress. Drift measurements settings: 120 minutes stress @ 5MV/cm electric field with intermediate V_c (collapse voltage) measurements.
Note 7: Centre frequency and bandwidth are derived from impulse response in immersion. On sample basis on a few devices from a batch. See for settings and typical

result Figure 9. These measurements were done on devices with full acoustic stack (version B) as shown in Chapter 3.4.

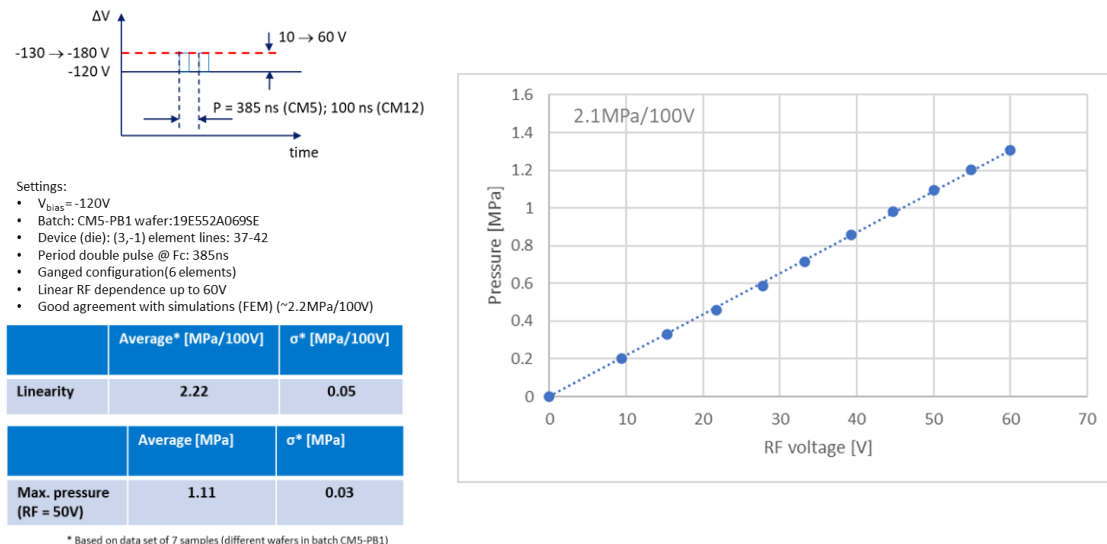*Figure 9: Impulse response result. Left: settings impulse response measurement and parameters derived from impulse response. Right: spectrum impulse response (average 5 samples) with definition centre frequency and band width (BW) at -3dB points.*
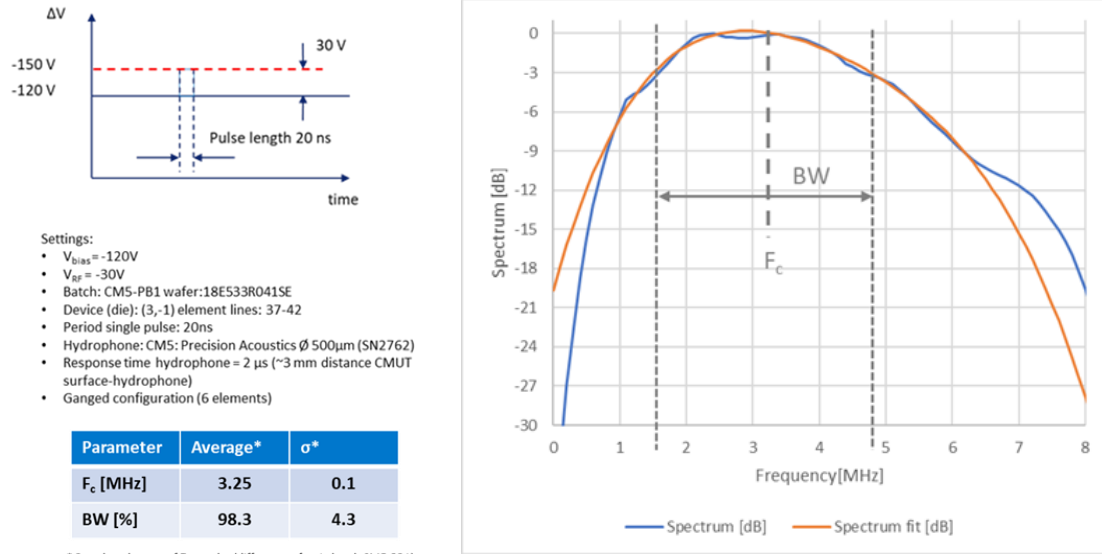
Note 8: Sound pressure measurements done on multiple channels with varying bias and RF voltages. The pressure is measured with calibrated hydrophone. On sample basis on a few devices from a batch. See for settings and typical result Figure 10. These measurements were done on devices with full acoustic stack (version B) as shown in Chapter 3.4.

Figure 10: Sound pressure as function of RF voltage at 120V bias. Left: settings of linearity measurement. Right: lineartity measurement

Note 9: Imaging specific requirements will only be investigated on sample basis during later development.

3.2 Transfer CMUT process to 200mm

The CMUT process is transferred from 150mm wafer size to 200mm wafer size. This is important for cost reduction. For the CM5 array shown in Figure 7, the number of devices per wafer doubles from ~35 towards ~70.

The main conclusions for the transfer to 200mm are:

➢ Same performance for 150mm and 200mm with good process capability (C_{pk}>1.67)

On collapse voltage, impedance, and acoustics:

➢ Collapse voltage (V_c) is a good process control parameter: both for mechanical and electrical performance. See Figure 11, for typical results on both 150mm and 200mm.
➢ Good yield on wafer level
➢ Narrow collapse voltage distributions for both 150 and 200mm (see Figure 11)
  ➢ σ~1V (~2%) for 150mm and ~2-3V (~4-5%) for 200mm
  ➢ 200mm → small increase in thickness and etch variations
  ➢ Variation in V_c has only small effect on acoustics and imaging → V_c is mostly a process control parameter
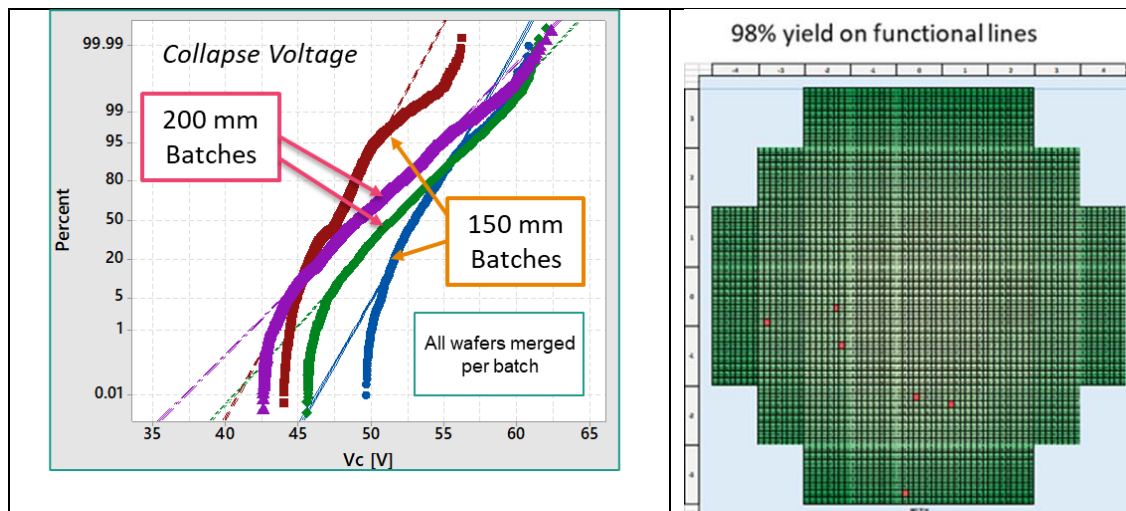

Figure 11: Left: probability plot comparing collapse voltage of the 200mm batches compared with 150mm batches. Right: wafer map showing yield on collapse voltage for all CMUT elements. Red dots indicate missing elements in CMUT array (opens/shorts).

3.3 Process sensitivity analysis (corner batches)

The process sensitivity was investigated, and the important process parameters are identified (critical to quality (CtQ)). The flow of such an investigation is shown in Figure 12. The process variation specifications were used as input for a finite element modeling (FEM) sensitivity analysis. This analysis showed that the acoustic performance is dominated by the following process parameters (CtQ parameters):

- Dielectric thickness
- Gap height (sacrificial metal)
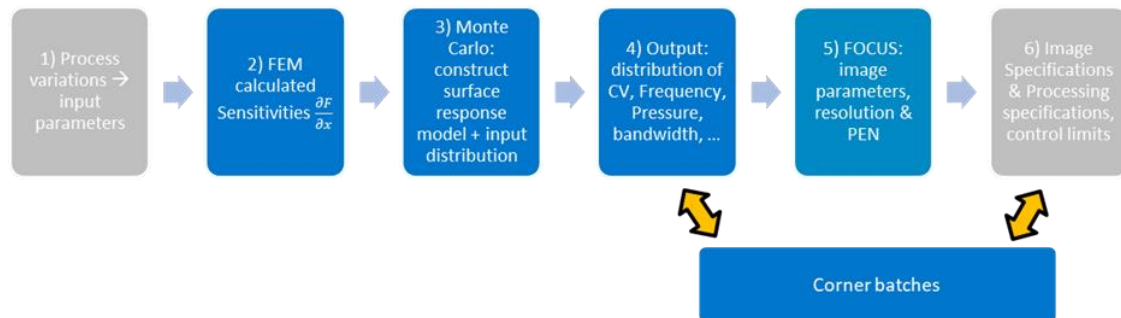- Membrane thickness (SiN layer)

Moore4Medical

Enabling "Moore for Medical"

Figure 12: Flow showing the different aspects of a process sensitivity investigation.

Box-Behnken experimental design was used to determine the response surface quadratic model → 3 batches with 3 factors (CtQ parameters). In Figure 13, the schematic x-section with the 3 factors is shown together with the design of experiments scheme. The variation in the CtQ parameters were +/- 10% of the reference value. This 10% variation in process parameters results in > ±5σ range, indicating a robust process window with C_{pk} > 1.67.
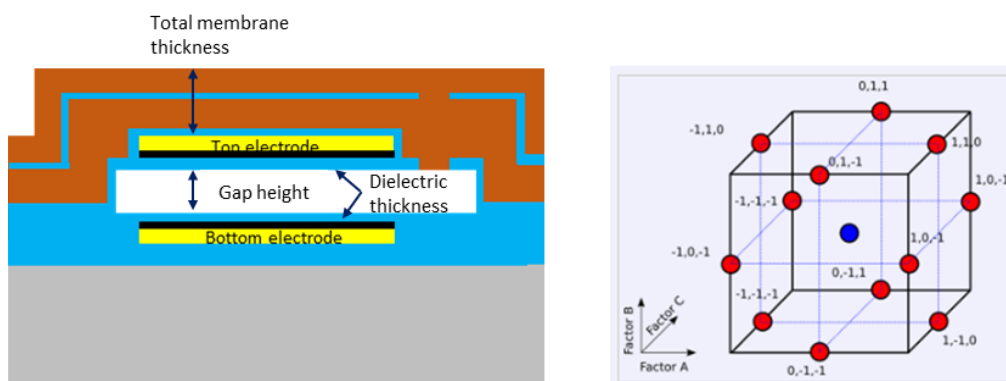
Figure 13: Left: Schematic x-section showing the three CtQ parameters. Right: Box-Bencken scheme for design of experiments.

The collapse voltage is an important parameter, because from all elements in all arrays on all the wafer this voltage is measured. The parameter is very sensitive for variation in all process parameters, like layer thickness, stress values and dimensions.

Figure 14: Collapse voltage (boxplot) for the different corners of the CtQ parameters

The variation of the collapse voltage for the 3 important CtQ parameters is shown in Figure 14. The corners of this Design of Experiments (DoE) spans collapse voltage variations from ~30V up to ~80V. In the graph also the typical (average) value of V_c for CM5 is shown together with 6σ limits. This shows that the corners of the DoE nicely covers more than ±6σ, indicating that corners are well chosen. The measured variation of the $V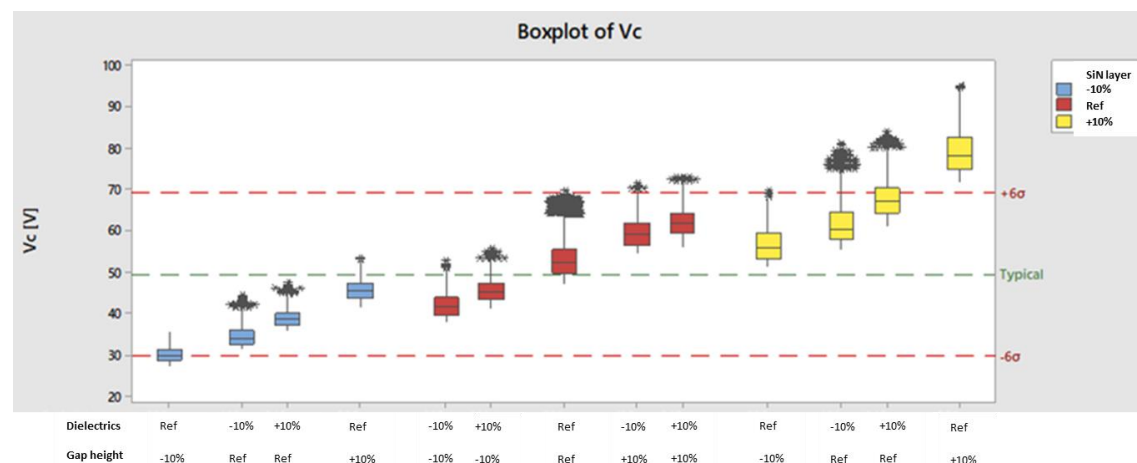_c$ fits well with the values obtained by FEM, as shown in Table 3. This good fit shows the accuracy of the simulations by FEM. FEM is also used to tune the CMUT device architecture for different applications (F_c, BW, pressure sensitivity).

Table 3: comparison V_c variation for CtQ parameters determined with FEM and measured.

	$\partial Vc/\partial x$ FEM	$\partial Vc/\partial x$ Measured
Gap height	0.22 V/nm	0.18 V/nm
Dielectric thickness	0.05 V/nm	0.05 V/nm
Membrane thickness (SiN)	0.019 V/nm	0.02 V/nm

In Figure 15, a typical example of acoustical measurement is shown for variation in gap height. An impulse response is shown for single line, showing small shift in spectrum between both variants. The hydrophone distance is ~3mm and spectrum is not corrected for diffraction effects. For increasing gap height, the centre frequency increases from 4.16 to 4.72MHz, relative bandwidth (BW) decreases from 98% to 85% and sensitivity from 2.10 to 2.16 MPa/100VRF. These changes are relatively small considered the large variation in gap height. The measurements were in line with the variations obtained with simulations.
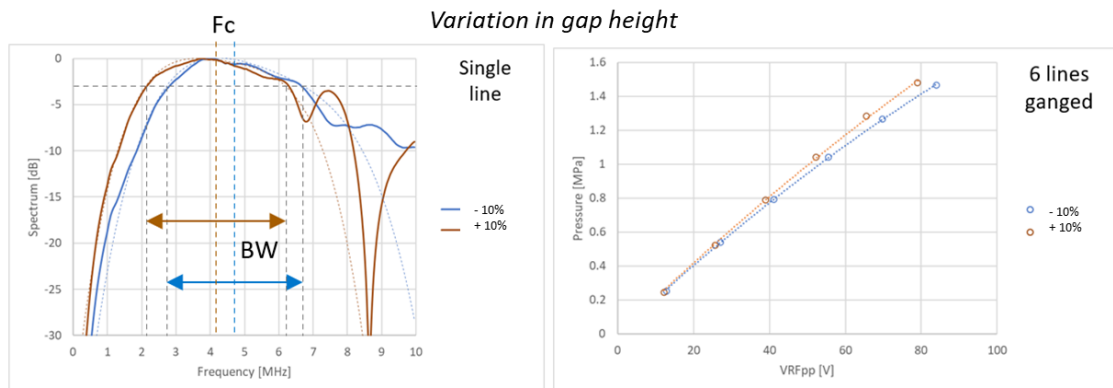
Figure 15: Left: impulse response results for two corners (+/- 10% gap height). Right: For the same corners the sound pressure as function of RF voltage.

The process corners only result in a relatively small variation in acoustics. See another example on pressure sensitivity shown in Figure 16. The probability plot shows all pressure sensitivities measured for all measured devices (reference and corners).
This sensitivity analysis showed that the low frequency CMUT process is robust. With process specification limits >5σ with resulting capability P_{pk}>1.67, only small variation in acoustics is observed. An overview of the variation in acoustics determined with the corner batches:
Total spread (mean±1σ)

Moore4Medical

Enabling "Moore for Medical"

WP4 D4.3, version 1.0
Moore4Medical
Ecsel-2019-1-876190
Page 20 of 44

- F_c = 4.31±0.28 [MHz]
- BW = 93.4±3.7 [%]
- Sensitivity P = 2.25±0.14 [MPa/100VRF]
- P_at_60VRF = 1.18±0.07 [MPa]

For all foreseen applications, these variations in acoustics have only minor influence on imaging and will be within specification.

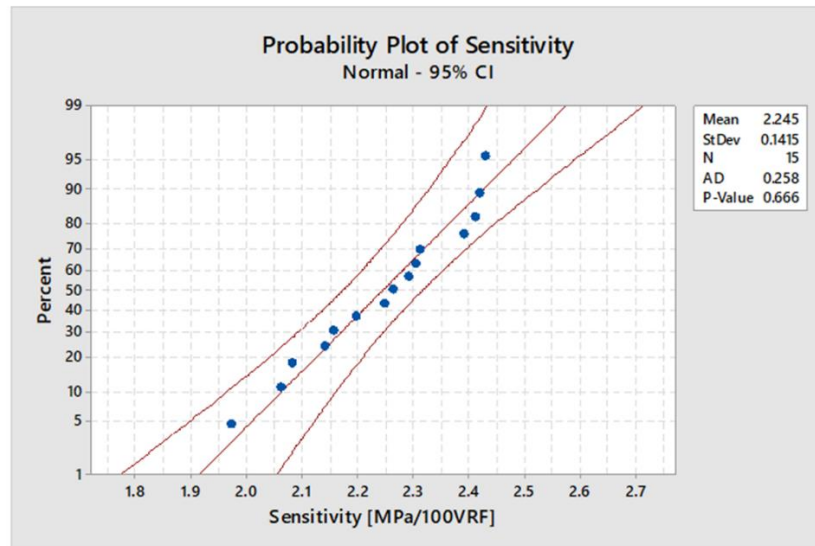*Figure 16: probability plot showing all pressure sensitivities (MPa/100V) measured for all process corners.*

3.4 Acoustic CMUT module development

For imaging, the CMUT device needs to be assembled into an acoustic module, including front side lens, and backing (minimizing reflections).
For the assembled devices, the following initial requirements are defined:
- Low leakage currents between different elements (<100nA)
- Good wire bond connection, resulting in no missing elements
- Shelf life at room temperature (RT) specification depends on application, but at least > 1 year
- Operational temperature (<40°C) and no water ingress, tested with accelarated aging at 60°C and 85%RH.
- Good imaging performance. This of course depends on the application, but the acoustic module should not result in clear imaging artefacts.

In Figure 17, different versions of our assembled CMUT devices are shown. Version A and B have the same acoustic stack and assembly method, with the only difference being the substrate. In version A, a flexible PCB was used, mainly for ease of use in our measurement and imaging setups, and in version B a rigid one. The transition from flex to rigid was needed to increase the robustness of the assembly. The flex solution suffered from wire bond breakage when too much stress was applied on the flex. This was solved by using a rigid PCB instead of a flex PCB. The PCB was protected with parylene-C coating to prevent water ingress. The acoustic stack and its manufacturing flow is schematically shown in Figure 18.

Moore4Medical

Enabling "Moore for Medical"

WP4 D4.3, version 1.0
Moore4Medical
Ecsel-2019-1-876190
Page 21 of 44

Figure 17: Three versions of assembled CMUT modules. Left: version A with CM5 and acoustic stack mounted on flex. Middle: version B, same acoustic stack mounted on PCB. Right: version C with improved assembly method and acoustic stack with PCB mounted in metal housing

The CMUT CM5 chip is thinned down to minimize the effect of reflections and attached to the PCB. The chip is wire bonded to the PCB with Al or Au wires. In the future different connection methods or flip chip options could be investigated. The wire bonds are protected with dam & fill with a polymeric soft material. A lot of effort is spent in finding the right material with optimizing the deposition and curing method. The protection of the wires is important for operation in wet environments. After dam & fill, the lens was glued to the chip. The TPX/PBR lens consists of an injection moulded component with a shape such that the CMUT array has a 5cm focal point in the elevation direction. The material combination was chosen for its hardness (TPX), integration on top of CMUT (PBR) and acoustic properties of both materials (low attenuation and good matching). A final seal was applied at the sides of the acoustic stack to protect the silicon die from the environment.

Figure 18: Left, version B: schematic assembly flow of the acoustic stack. Right: CMUT CM5 device assembled on PCB

Initially, this version showed promising results but degraded over time. The assembled devices suffered from moisture intake, resulting in limited shelf life. Also, water ingress during long measurements in a water tank resulted in breakdown. The dam & fill polymers absorb water and stress resulted in delamination and wire bond breakage. The same issues were observed during aging test at 60°C and 85%RH. Another issue was the limited robustness of the parylene-C coating of the PCB, mainly due to scratches.
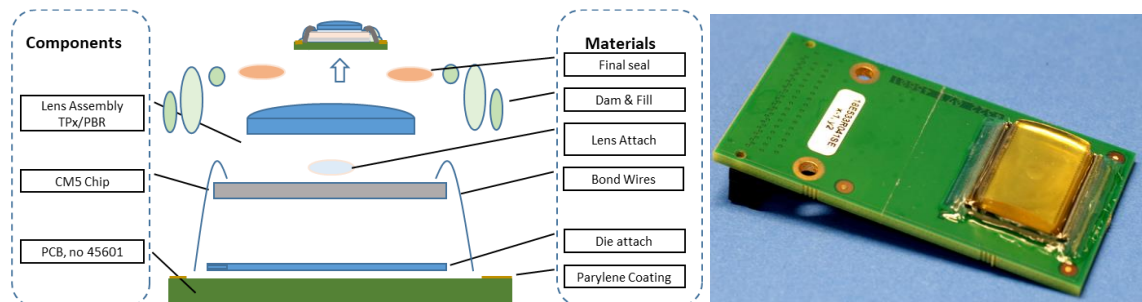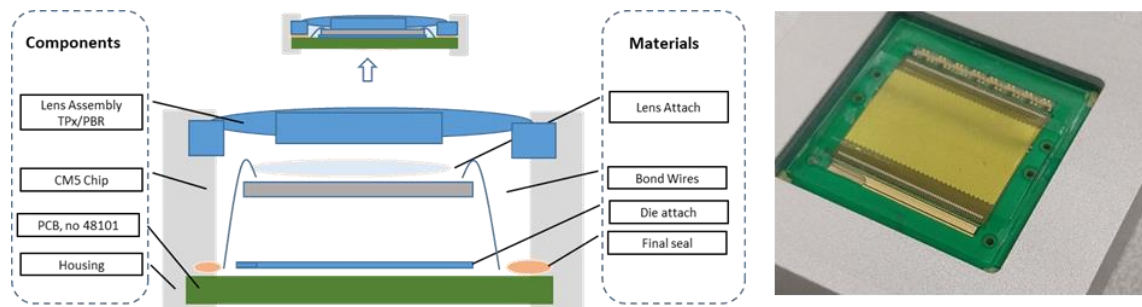

Figure 19: version C: schematic assembly flow of the acoustic stack. Right: CMUT CM5 device assembled on PCB within metal housing.

A new version C was designed to solve these issues. The main improvements were the use of a larger lens with cavities for the wire bonds. This eliminates the requirement for dam & fill to protect the wire bonds for water ingress. Either no dam & fill or softer dam & fill polymers can be used. The PCB is mounted in a metal housing, pressing the lens onto the PCB with a silicone gasket. These assembled devices can be used by internal and external customers of Philips MEMS & Micro Devices for application development. Later, the metal housing can be replaced by e.g., a dedicated probe design.

With assembled low frequency CMUT CM5 arrays, imaging was done with the Philips Lumify system. For the imaging test with a wire phantom, the standard probe as shown in Figure 20 (curved probe Lumify: ceramic piezo) was replaced with the CM5 PCB. The maximum focus depth and penetration depth of the Lumify system is 24cm. A typical example of an image with CM5 (V_{bias}: 120V; V_{RF}: 50V) showing the wire phantom is shown in Figure 20. The images taken with CM5 array were not post processed and the Lumify settings were not optimized for CM5. Further improvements in both penetration depth and image quality can be expected with tuning of the Lumify settings for CMUT instead of piezo.
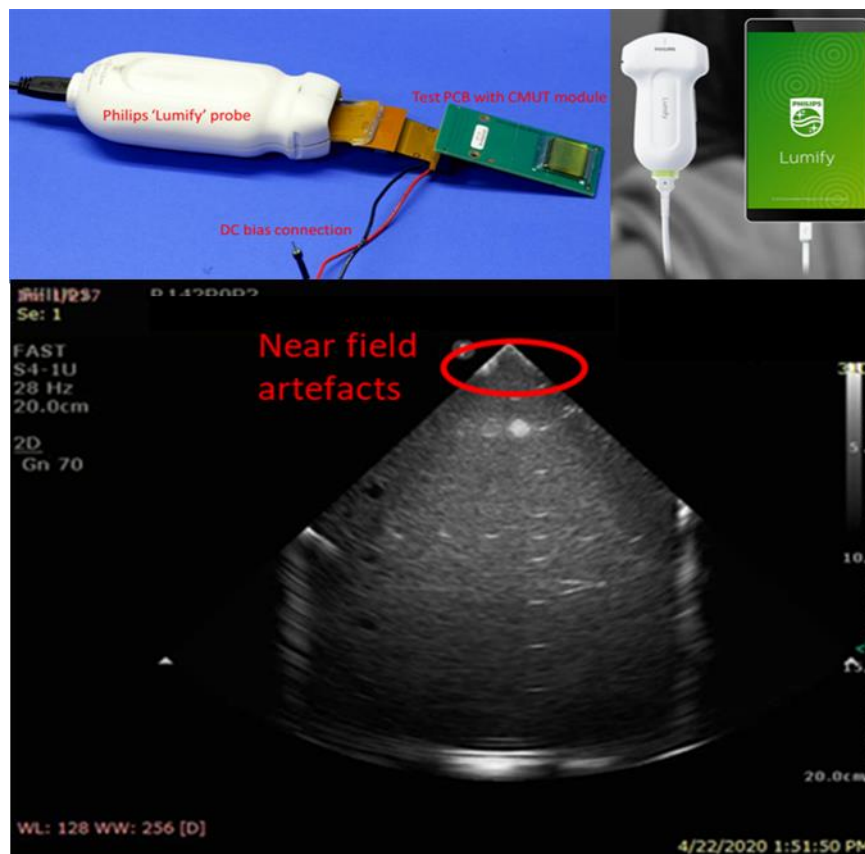
Figure 20: Top: 'Lumify' probe is used for first imaging test with low frequency CMUT module. Bottom: image taken with CMUT probe shown, resulting in some near field artefacts.

3.5 Low voltage CMUT variants

A disadvantage of low frequency CMUT CM5 devices is the high bias voltage of 120V, needed for operation in collapse mode, in combination with RF voltages up to ±50V. It would be advantageous if the devices could operate with lower voltages. If the total voltage is below 60V, electrical isolation will be easier for use on the body (probe or patches). Also, integration with ASIC will be easier due to the limited voltage up conversion. The main tuning for low voltage operation is scaling down of the dielectrics.

Moore4Medical

Enabling "Moore for Medical"

In Figure 21, the scaling of the dielectric thickness is shown together with the operational voltages. Next to this the full device architecture is tuned for optimized performance.

Standard: dielectric: 200nm	Dielectric: 100nm	Dielctric: 60nm
DC bias: 120V	DC bias: 60V	DC bias: 35V
RF: 50V	RF: 30V	RF: 20V

Figure 21: Scaling of dielectrics and voltages

For the optimization of the devices, FEM was used and in Table 4 the performance parameters of the different variants are summarized. It shows that the low voltage variants have better performance (round trip, pressure sensitivity and maximum pressure) combined with lower operational voltages. The roundtrip value is the multiplication of the sensitivity times maximum pressure. It is based on the observation that receive and transmit sensitivities are linked. Increase in transmit sensitivity results in an increase in receive sensitivity. The processing of the low voltage variants is slightly different compared to the standard version, mainly due to the lower gap height resulting in more challenging etching of sacrificial material (see Figure 5 E). The process window might be smaller than shown in Section 3.3. The sensitivity analysis done with corner batches for the standard design needs to be repeated for the low voltage variants.

Table 4: Properties of standard and low voltage variants CMUT (CM5)

Properties	Standard CM5	Low voltage CM5	Ultra-low Voltage CM5
Bias voltage [V]	120	60	35
Round trip	2.0	4.85	4.77
Max RF [V]	+50, ±30	±30	±20
Fc [MHz]	3.0	3.1	3.2
BW [%]	112	116	116
Sens. [MPa/100V]	1.84	2.85	3.41
Max. Pressure [MPa]	1.1	1.7	1.4
Dielectric thickness [nm]	200	100	60

The sound pressure measurement results are shown in Figure 22. The low voltage and ultra-low voltage devices operate with the lower voltages, but the performance gains are lower than expected from FEM.
The sensitivity for the different variants for both simulations and measurements are:
- – Standard HV:
  - • Measured: sensitivity: ~2.3MPa/100V
  - • FEM: 1.84MPa/100V
- – LV:
  - • Measured: ~2.6MPa/100V
  - • FEM: 2.85MPa/100V
- – ULV:
  - • Measured: ~2.8MPa/100V
  - • FEM: 3.41MPa/100V

Some process optimization and tuning are needed to further improve the performance. A new batch with process tuning is currently in progress.

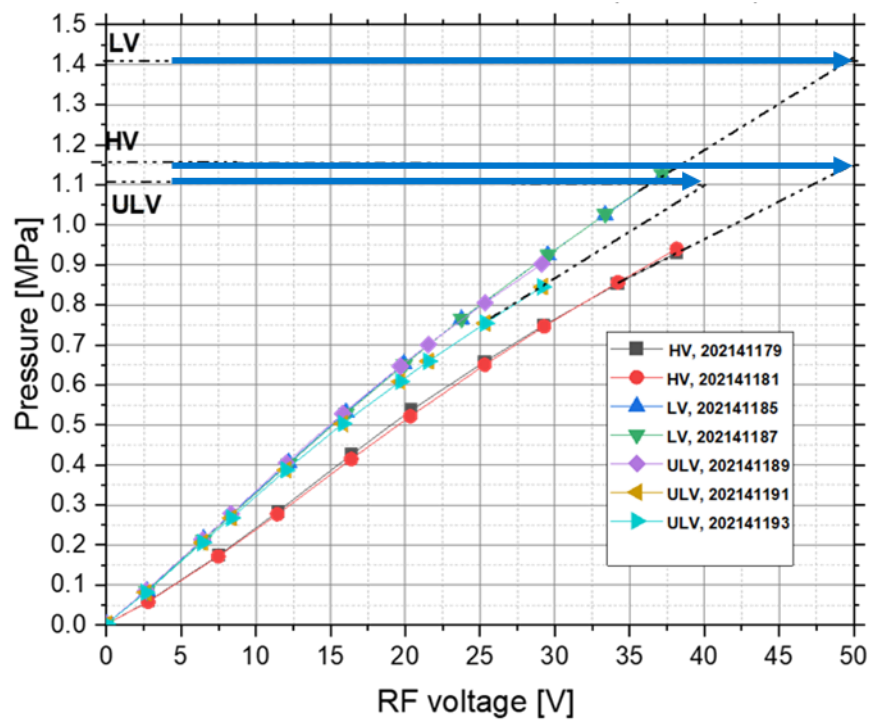**Moore4Medical**

Enabling "Moore for Medical"

Figure 22: Sound pressure as function of RF voltage for standard 'high voltage' (HV), 'low voltage' (LV) and 'ultra-low voltage' (ULV) variants. The arrows and dash-dotted lines indicate the extrapolation to maximum RF voltage.

4 Low frequency PMUT development

This section describes the development of a 64-element 1-D PMUT array prototype, including the design, fabrication, packaging, system integration, and testing.

4.1 Design

The 1-D PMUT array has been designed around low-frequency ultrasound imaging requirements, focusing on both diagnostic (e.g. cardiac and abdominal) and non-professional (e.g. fetal monitoring) applications. The geometrical specifications and the electro-acoustic design parameters of the array, summarized in Table 5, have been defined in the frame of the earlier EU project POSITION II [5].

Table 5: 1-D PMUT array design parameters

Parameters	Target	Unit	Notes
Geometric			
Number of elements	64		
Pitch	300	µm	
Elevation	12	mm	
Electro-acoustic			
Centre frequency	3	MHz	1
Fractional bandwidth	>70	%	1
Transmit sensitivity	20	kPa/V	2
Maximum transmit pressure	1	MPa	3
Maximum AC voltage	60	V	3
Maximum DC voltage	60	V	

Note 1 - Frequency band defined for transmit operation; parameters defined at -3dB.
Note 2 - Transmit sensitivity value is at centre frequency.
Note 3 - Maximum pressure and voltage values are peak-to-peak. Pressure is defined at the transducer surface.

The PMUT microstructure and layout have been designed using Finite Element Modeling (FEM). A FEM model of the PMUT microstructure, consisting of a multi-layer membrane supported by a silicon substrate and suspended over a cavity has been established. The microstructure design has been approached iteratively by varying the geometric parameters within the ranges allowed by the STM sol-gel PMUT process design rules, and by computing the electro-acoustic transmit and receive responses. The PMUT modelling included the presence of the typical package elements, i.e., the backing and the front encapsulation layers, whose aim is to minimize the effects of spurious vibration modes of the package on the electro-acoustic response. The PMUT cell layout was defined considering the rectangular array element dimensions of 300 µm by 12 mm. Figure 23 shows the FEM simulated two-way electro-acoustic frequency response, which is centered at 2.7 MHz with a -6dB fractional bandwidth of 80%. Each array element is composed of 184 circular PMUT cells connected in parallel, resulting in 11776 cells in total. As the element capacitance is relatively high, FEM was also used to model the PMUT electrodes and routing traces to minimize and to equalize the top and bottom electrodes' parasitic series resistance. Iterative simulations were run to determine the optimal widths of the top and bottom electrode traces. Figure 23 (bottom) shows a detail of the final mask layout, with top and bottom electrodes highlighted, onto

Moore4Medical

Enabling "Moore for Medical"

which contour plots of the FEM-simulated electrical current density flowing through the top and bottom electrode traces with a DC voltage applied are superimposed. The mask layout for the fabrication of the PMUT array was then designed considering both the geometrical parameters of the PMUT microstructure (i.e., cell diameter and position, piezoelectric element diameter, and electrodes shape) optimized by simulation, as well as the requirements of the packaging flow established for electrical interconnection, backing and encapsulation. Figure 23 shows the resulting mask layout of the die, which has an overall size of 21x15 mm, whereas the acoustically active area is 19.2x12 mm.
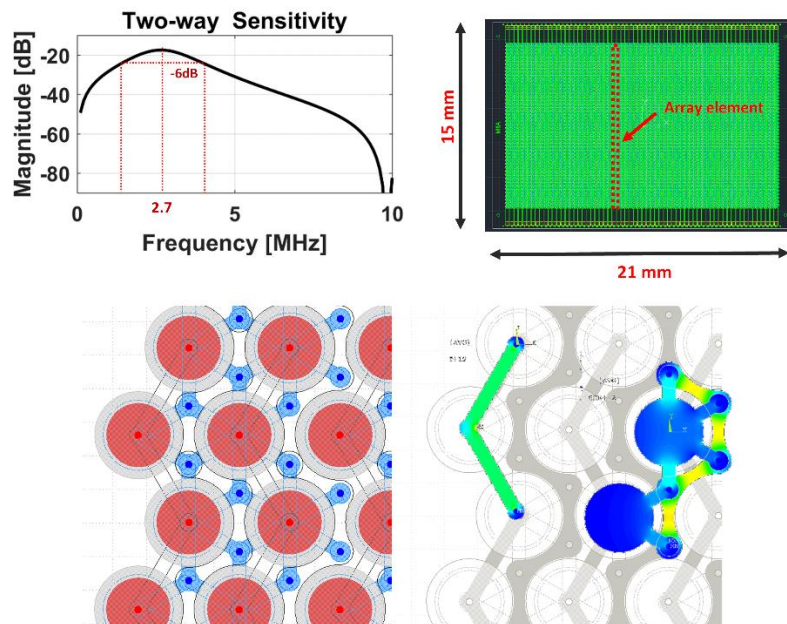

Figure 23: Design of the PMUT array: (top-left) FEM simulation of the two-way sensitivity; (top-right) geometrical layout of the die; (bottom) geometrical detail of the top and bottom electrodes layout and FEM simulation of the current density in the routing metal layer.

4.2 Microfabrication technology

The 1-D PMUT array has been fabricated using a sol-gel Lead Zirconate Titanate (PZT) thin film-based MEMS process from STMicroelectronics. The PMUT process is executed on a single 200mm wafer and is mainly composed by a front-side patterning to realize the silicon elastic plate layer, the PZT piezoelectric layer, and the relative electrical connections, and a backside cavity etching to release the membranes. Different operating frequencies can be obtained with a tailored design by mainly choosing the membrane lateral dimensions and thickness without the need of process customization. The fabrication process steps are summarized in Figure 24: the elastic plate layer consists of an oxide-silicon-oxide stack formed onto a silicon wafer (a), on top of which the bottom electrode, the sol-gel PZT layer, and the top electrode are deposited and patterned (b); the stack is then passivated, and a routing metal is deposited and patterned (c); the wafer thickness is then reduced, and the cavities are formed by etching the silicon from the backside (d).
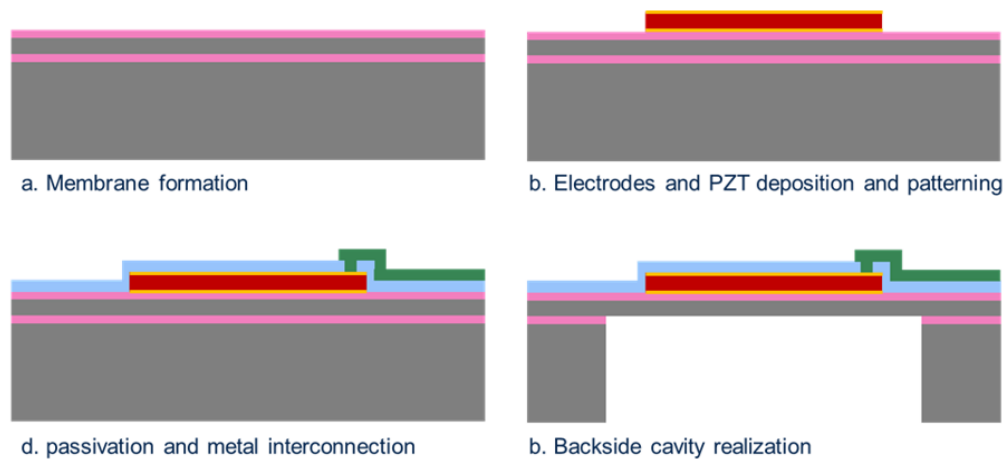
Moore4Medical

Enabling "Moore for Medical"

a. Membrane formation

b. Electrodes and PZT deposition and patterning

d. passivation and metal interconnection

b. Backside cavity realization

Figure 24: PMUT microfabrication: schematic description of the process flow

Figure 25 shows a picture of the fabricated PMUT array die and an optical microscopy of a detail of the PMUT cell layout seen from the top side of the die, where the top, bottom, and interconnection metals as well as the circular piezoelectric elements are clearly visible. It must be noticed that the edges of the circular membranes are not visible, as they are defined by etching of the cavities from the back side of the wafer.
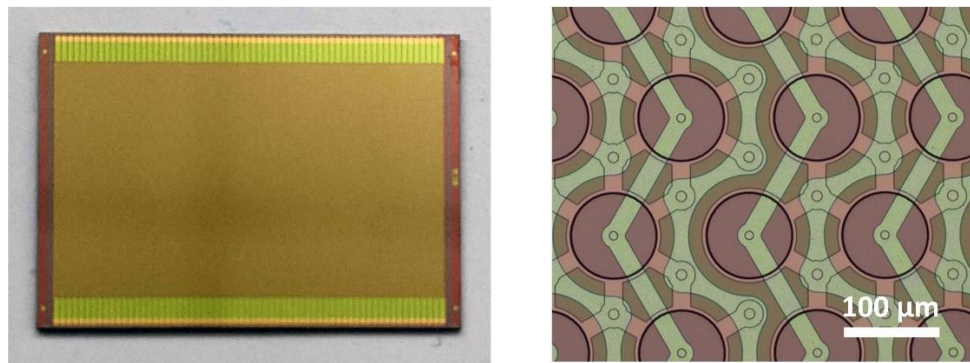

Figure 25: PMUT microfabrication: (left) picture of the fabricated 64-element PMUT 1-D array; (right) detail of the PMUT cell layout.

4.3 Array packaging

The fabricated array was packaged using the process defined during the first year of the Moore4Medical project. The general aim of the packaging process is to make the array easily connectable to electronic boards for basic electrical and acoustic characterization and for imaging testing. Such goal is achieved by electrically interconnecting the PMUT array to a rigid-flex printed circuit board (PCB), and by providing the resulting assembly with suitable backing and encapsulation elements.

The rigid-flex PCB and the PMUT array are schematically diagramed in Figure 26. The rigid-flex PCB consists of a central flexible part made of Polyimide (PI) hosting an aperture used to host the PMUT array, and two lateral rigid parts made of FR4 used to connect the PMUT elements to external boards.

Moore4Medical

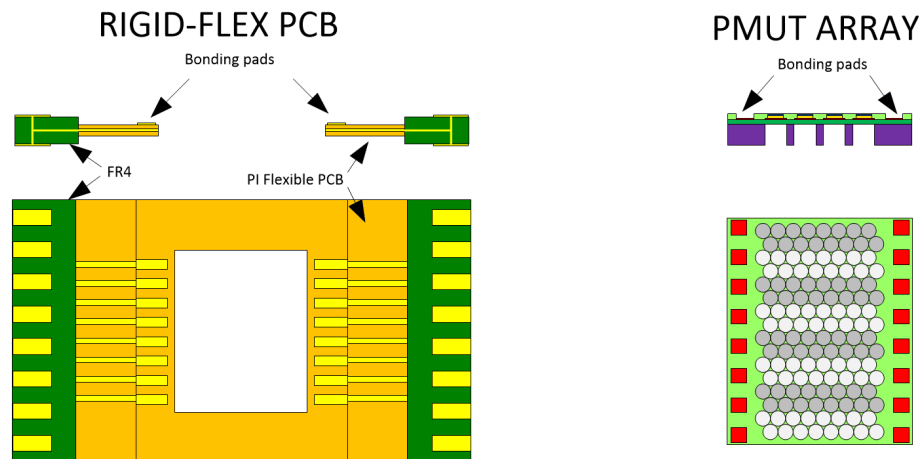Enabling "Moore for Medical"

Figure 26: Simplified schematic top and cross-section views of the PMUT array die (right) and of the rigid-flex PCB (left): the PCB has a central PI part including aperture to hosts the PMUT array, and two lateral FR4 boards to connect the array to external boards.

The packaging process flow previously developed is reported in Figure 27. With reference to the figure:

A: The PMUT die is aligned to an FR4-Polyimide rigid-flex PCB. Wire bonding is used to connect the PMUT to the rigid flex PCB. An epoxy-based glob top encapsulant material is then applied to protect and insulate the wires and to provide mechanical stability to the packed chip.

B: A pre-shaped backing is attached to the bottom side of the PMUT die in correspondence of the active area using an acrylic adhesive at ambient pressure. An elastomeric front encapsulation layer, which acts as an acoustic window for acoustic matching, insulation, and protection, is finally applied.

C: The rigid-flex PCB is bent and fixed to the package. The resulting assembly, here referred to as a probe head, may be connected to external boards, such as characterization circuits or in-probe PCBs, hosting receive (RX) low-noise amplifier (LNA) integrated circuits (ICs).
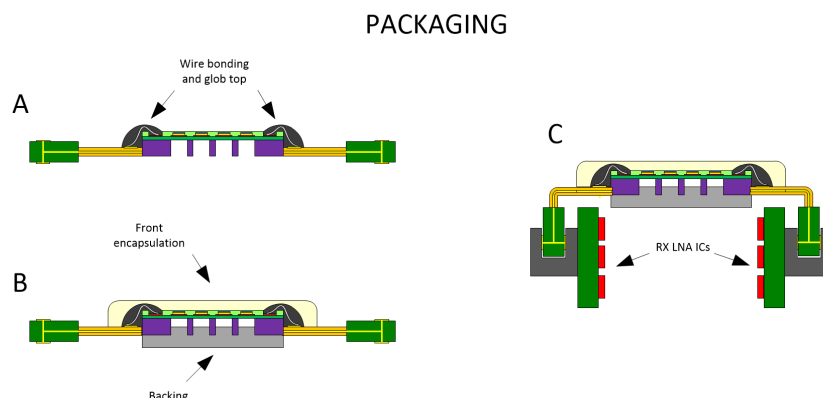

Figure 27: Simplified schematic diagram of the PMUT array packaging process: Wire bonding of the PMUT array to the rigid-flex PCB and glob top encapsulation (A); backing application and front encapsulation (B); flexible circuit bending and connection to external boards (C).

The described process was used to fabricate a prototype PMUT probe head. The electrical interconnection was performed by Al wire bonding and glob top encapsulation.

The PMUT array was hot-poled by applying a DC voltage of 40 V at a temperature of 150 °C for 8 hours. An epoxy resin (EPO-TEK 301, Epoxy Technologies Inc.) block filled with tungsten and alumina powders, and an elastomeric silicone-based flat layer were applied for the acoustic backing and front encapsulation of the PMUT, respectively. Figure 28 shows pictures of the main steps of the PMUT array packaging process.
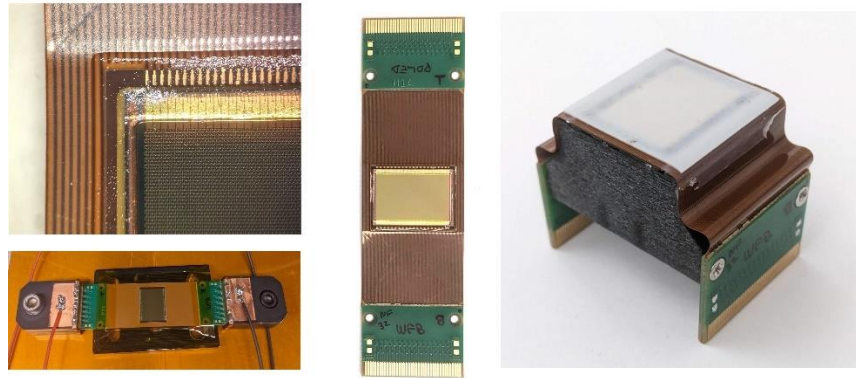

Figure 28: PMUT array packaging: detail of the wire bonding of the array to the rigid-flex PCB and glob top encapsulation (top-left); bonded PMUT array connected to the poling fixture (bottom-left); overall view of the PMUT array bonded to the rigid-flex PCB; final prototype probe-head achieved by applying the backing and front encapsulation layer.

4.4 System integration and testing

The PMUT array was characterized at different stages of the packaging process. An electro-mechanical characterization has been carried out to extract the main electrical and mechanical characteristics of the PMUT array elements in air-coupled condition to assess the die-level uniformity and parasitic elements, and to determine the ideal biasing and driving conditions. The PMUT probe head has then been integrated into an ultrasound probe to carry out an electro-acoustic characterization in water-coupled condition to extract the main figure of merits and perform preliminary in vitro imaging tests.

4.4.1 Electro-mechanical characterization

The PMUT array electro-mechanical characterization started with Laser Doppler Vibrometry, consisting in measuring the displacement of the centre of one PMUT cell operating in air, i.e., before applying the front encapsulation layer. The plots shown in Figure 29 (bottom-left) report the displacement sensitivity spectrum of a cell located in the centre of the die. The same measurement has been performed before and after poling by sweeping the DC bias voltage. From the displacement spectra, the low-frequency (500 kHz) magnitude has been extracted and plotted as a function of the bias voltage. Figure 29 (bottom-right) shows the low-frequency displacement magnitude plotted as a function of the bias voltage before (blue) and after (red) poling. The blue curve, achieved before poling, shows the expected nonlinear behavior related to PZT ferroelectric properties in the -60V-to-60V range, while the red curve, achieved after poling, shows that the electro-mechanical response becomes nearly linear in the 10-to-70V range. These results have allowed establishing optimal biasing and driving conditions of the array, with respect to the PMUT linearity, resulting in maximum DC and AC voltages of 40 and 30 volts, respectively.
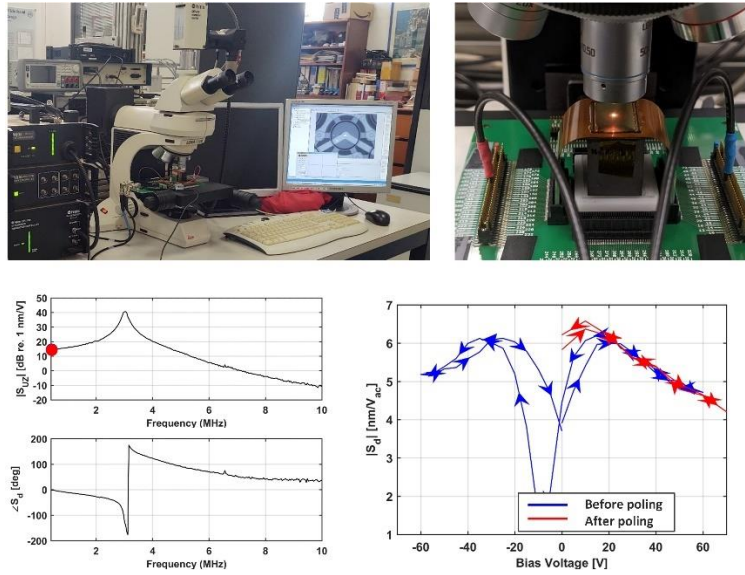
Figure 29: Electro-mechanical characterization of the PMUT array: Laser Doppler Vibrometry setup (top); magnitude and phase of the displacement sensitivity spectrum (bottom-left); low-frequency displacement sensitivity magnitude plotted as a function of the bias voltage (bottom-right) before (blue) and after (red) poling.

Air-coupled electrical impedance measurements have then been carried out on all the array elements to assess the basic array characteristics and uniformity. The plots shown in Figure 30 report the impedance measurement results for all 64 elements of a poled array biased at 40 V. From these data, element capacitance and resonance frequency have been extracted. The mean capacitance is 2141 pF with a relative standard deviation (RSD) of 0.87 %, and the mean resonance frequency is 3.1 MHz with a RSD of 0.59 %. Parasitic elements have also been extracted from the impedance data. The series resistance of the PMUT electrodes is 11.5 Ω, whereas the series inductance, mainly introduced by the rigid-flex PCB is 254 nH. The parallel resistance is in the order of a few GΩ and therefore neglectable.
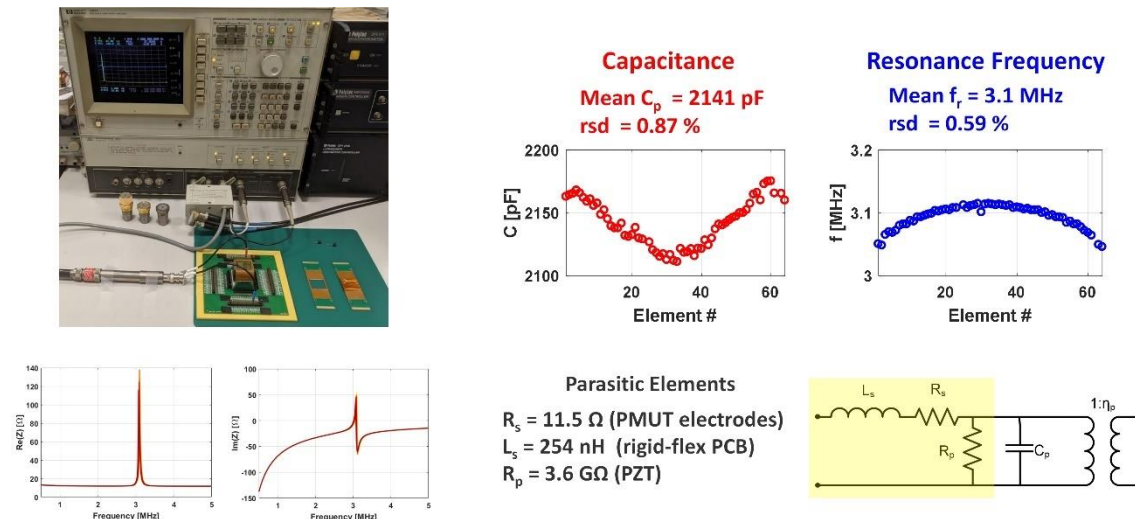

Figure 30: Electro-mechanical characterization of the PMUT array: electrical impedance measurement setup (top-left); electrical impedance spectroscopy (bottom-left) of 64 array elements; extracted element capacitance and resonance frequency (top-right); parasitic equivalent circuit (bottom-right).

4.4.2 Probe development

The PMUT probe head has been integrated into an ultrasound probe to allow the connection to the ULA-OP 256 scanner [12] for electro-acoustic characterization and imaging assessment. The probe includes an electronic board comprising 64 low-noise voltage amplifiers (LNAs, MAX14822, Maxim Integrated Products) featuring high input impedance and programmable gain. The in-probe 64-channel board host the LNAs and the power management circuits for the control of the power supplies and the PMUT voltage biasing, which is fed to each of the array elements through an R-C bias-tee. The probe is connected to the ULA-OP 256 scanner using a multi-conductor cable, comprising micro-coaxial cables for the analog and digital signals, as well as dedicated cables for power supply and biasing voltages. The ULA-OP 256 scanner has been equipped with a custom control board dedicated to the power supply and configuration of the probe. The final probe assembly has been housed inside a 3-D-printed ergonomic probe handle for waterproofing and electromagnetic shielding. Figure 31 shows pictures of the developed in-probe electronic board, of the prototype probe, of the scanner, and of the active probe control board.
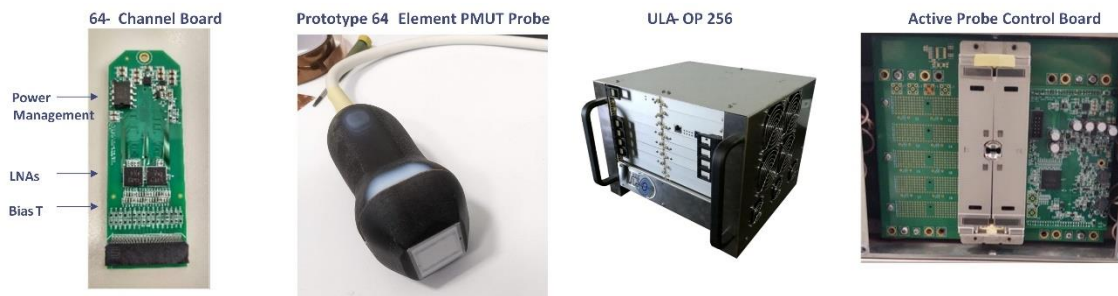

Figure 31: Pictures of the developed probe and scanner. From left to right: in-probe 64-channel electronic board including LNAs and power management circuitry; assembled 64-element prototype probe; ULA-OP 256 scanner; probe connector, and active probe control board.

4.4.3 Electro-acoustic characterization

Electro-acoustic characterization has been carried out using the PMUT probe in conjunction with the ULA-OP 256 scanner in a water tank setup, as shown in Figure 32. The front part of the probe, i.e. the packaged PMUT array, is partially immersed in water facing downwards. The water tank setup is equipped with a precision 3-axis motorized stage used to hold and move an immersed hydrophone or planar reflector for acoustic pressure and pulse-echo measurements. The setup allows precise adjustment of the position of the hydrophone and reflector relatively to the transducer, thus ensuring accurate alignment. Small signal characterization has been carried out to extract the transmit (TX) and receive (RX) sensitivities, and the two-way (roundtrip) fractional bandwidth, while large signal measurements have been performed to assess the maximum pressure, the linearity, and the harmonic distortion.
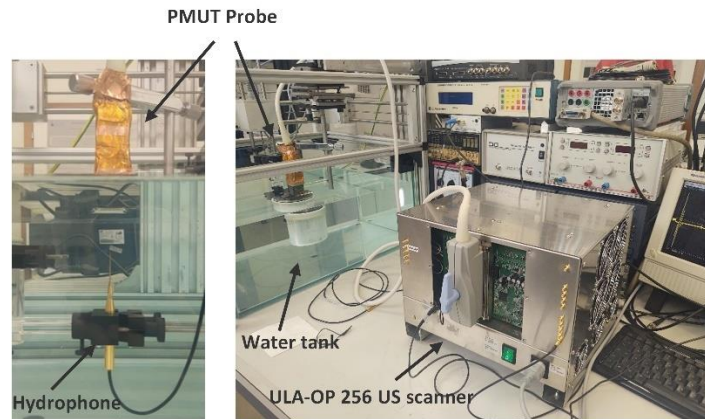
Moore4Medical

Enabling "Moore for Medical"

Figure 32: Water tank setup used for the electro-acoustic characterization.

Small signal acoustic characterization of the 1-D PMUT array has been carried by performing TX pressure and pulse-echo experiments. The ULA-OP 256 scanner has been programmed to excite 4 adjacent PMUT array elements with a broadband signal consisting in a 10MHz, raised cosine pulse with an amplitude of 5 V. The TX pressure impulse response has been acquired at 36 mm from the transducer surface using a 0.2mm-diameter needle hydrophone (NH0200, Precision Acoustics, UK). The echo signal from a stainless-steel planar reflector placed at 18 mm was acquired at the system front end input using an oscilloscope. TX and pulse-echo impulse responses were Fourier transformed and numerically compensated for excitation, diffraction, absorption, and for the LNA voltage gain to estimate the TX and RX sensitivities at the transducer surface. TX and RX peak sensitivities and bandwidths have been extracted and compared with the FEM simulations results. Figure 33 shows the acquired hydrophone and pulse-echo signals, as well as the one-way TX, one-way RX, and two-way sensitivities estimated at the transducer surface. Peak TX and RX sensitivities are found to be around 31 kPa/V and 3.2 mV/kPa, respectively, and the two-way fractional bandwidth is 81 %, centered at 2.5 MHz. The results are consistent with the design specifications in terms of centre frequency and bandwidth. Measured and simulated RX peak sensitivities are practically coincident, while the measured TX sensitivity is around 3 dB lower than the simulated one because of the effects of the parasitic series inductance and resistance, not accounted for in the FEM models.
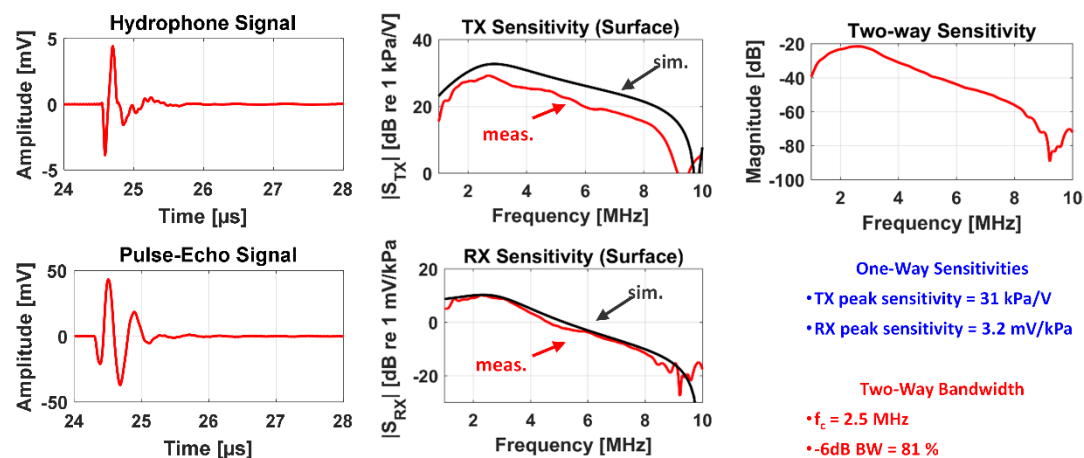

Figure 33: Small signal electro-acoustic characterization results: acquired hydrophone and pulse-echo signals (left); simulated and measured TX and RX sensitivities at the transducer surface (centre); measured two-way frequency response (right).

Moore4Medical

Enabling "Moore for Medical"

Large signal acoustic characterization of the 1-D PMUT array has been carried out by exciting 4 adjacent array elements biased at 40 volts, with a 2MHz, 10-cycle, Hanning-tapered, sinusoidal burst. TX pressure signals have been acquired at 10 mm from the transducer surface using a 0.2mm-diameter needle hydrophone. Several acquisitions have been carried out by sweeping the excitation amplitude from 10 to 30 volts with a 5 volts step. The pressure at the transducer surface was achieved by numerically compensating the hydrophone signals for diffraction and attenuation. The plots in Figure 34 show the acquired signals and their spectra, as well as the peak-to-peak surface pressure amplitude as a function of the excitation signal amplitude, and second harmonic distortion as a function of the peak-to-peak pressure amplitude. A maximum pressure of 1.8 MPa with a -22 dB second harmonic level was achieved with a 30V excitation amplitude, whereas a pressure of 1 MPa with a -30dB second harmonic-to-fundamental ratio (HFR), which is the typical harmonic distortion specification required for harmonic imaging, was achieved with a 22V excitation amplitude.
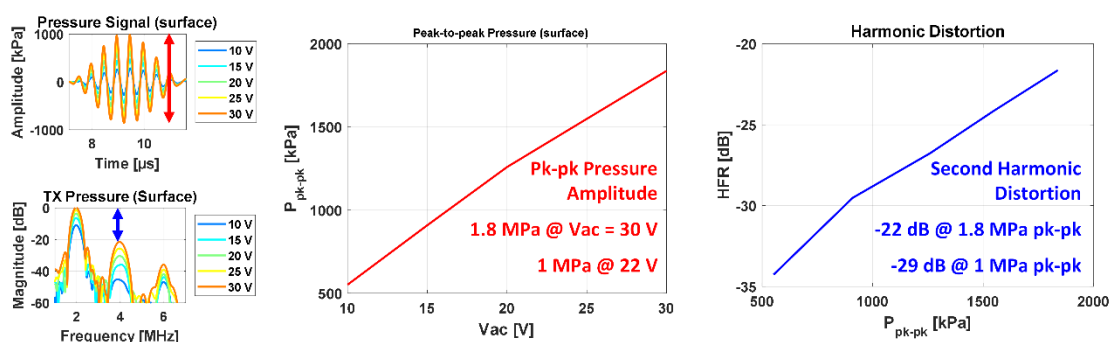

Figure 34: Large signal electro-acoustic characterization results: TX pressure signal and spectra at the transducer surface (left); Peak-to-peak pressure amplitude vs. excitation signal amplitude (centre) and second harmonic-to-fundamental ratio (HFR) vs. peak-to-peak pressure amplitude (right).

4.4.4 Imaging assessment

In vitro ultrasound imaging experiments have been performed in the setup shown in Figure 35 that included the prototype PMUT probe connected to the ULA-OP 256 scanner and coupled to a multi-purpose tissue-mimicking phantom (040GSE, CIRS). A sectorial scan of a portion of the phantom containing grayscale and wire targets at various depths has been carried out using 2MHz, 22V, 2-cycle, Hanning-tapered sinusoidal excitation pulses. Figure 35 shows examples of in vitro B-mode images, in which all phantom features, including both grayscale and wire targets, were clearly detected up to a 16-centimeter depth and distinguishably rendered with good contrast and axial resolution.

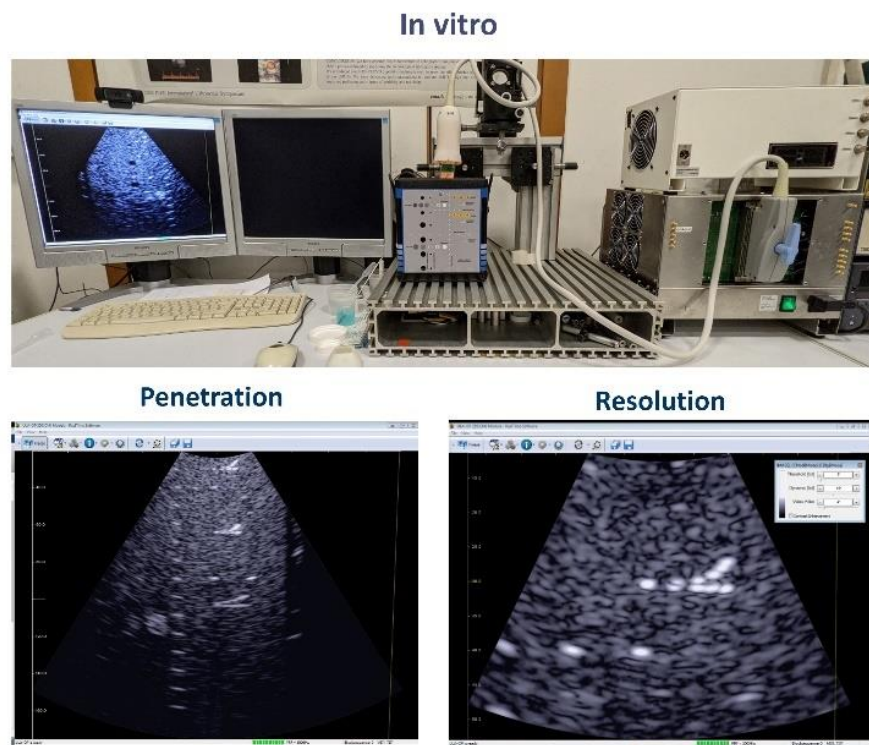**Moore4Medical**

Enabling "Moore for Medical"

Figure 35: Imaging assessment: Experimental setup (top); B-mode sectorial scans of a tissue-mimicking phantom (bottom) showing penetration (left) and resolution (right) capabilities of the PMUT probe.

5 Benchmark PMUT-CMUT

5.1 Benchmark results measured at Philips

5.1.1 Measurement setup

The benchmark measurements were performed with the same set up and settings as done for another EU project 'POSITION-II' [10]. That benchmark investigation was done with both PMUT and CMUT devices. The Philips CMUT device was already part of this comparison, but the ST PMUT was not. A difference with the earlier benchmark was the acoustic/protection layer on the array. In POSITION-II a PDMS/parylene layer was used and here we selected a PBR layer. The thin layer of PBR attenuates less than the PDMS/parylene stack and better comparison to real device performance can be made.
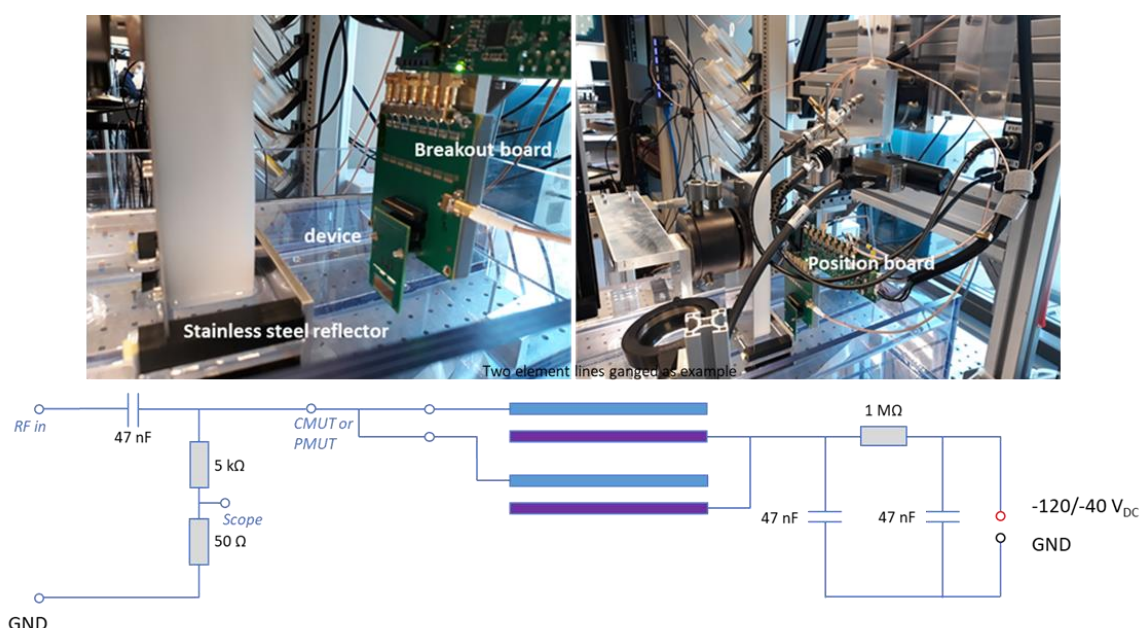

Figure 36: Top: measurement set up with water tank with immersed device and reflector for pulse-echo measurements. Bottom: electrical connection scheme for measurements. The bias voltage is -120V for CMUT and -40V for PMUT.

In Figure 36, the measurement set up and connection scheme is shown. The 'RF in' connection is connected to the so-called POSITION board. This was also used in the earlier benchmark and contains the transmit and receive electronics. The only change on the POSITION board was that the receive amplifier changed to high input impedance (10kΩ). For both PMUT and CMUT this high input impedance results in negligible influence of the electronics and good comparison is possible.

Other characteristics of measurement set up:
- Transmit: hydrophone 500µm.
- Pulse-echo: metal reflector
- Drive 6 channels/lines (linearity measurement) or 1 channel/line (impulse measurement)

Table 6: Measurement settings for benchmark

	lines	measurement	Bias PMUT	Bias CMUT	RF	driving	f	Cycles	Pulses	distance	Distance D²/4λ
Impulse	1	Transmit pulse echo	40V	120V	+15V	unipolar	25 MHz	0.5	1	10 µs	-
Linearity	6	Transmit	40V	120V	±5 to ±30V	bipolar	2.6 MHz	2	4	2 µs	41.6 µs
Linearity	6	Pulse-echo	40V	120V		bipolar	2.6 MHz	2	4	-	20.8 µs
Linearity	1	Pulse-echo	40V	120V		bipolar	2.6 MHz	2	4	-	20.8 µs

5.1.2 Pulse-echo impulse response

The acoustic pulse echo measurements were done with a metal reflector in the near-field (NF) as close as possible to the surface of the device under test and at a far-field (FF) distance. The impulse response measurement was performed with a unipolar single 20 ns pulse at NF and FF. The pulse is always additive to the applied DC voltage. A typical example for FF is shown in Figure 37.
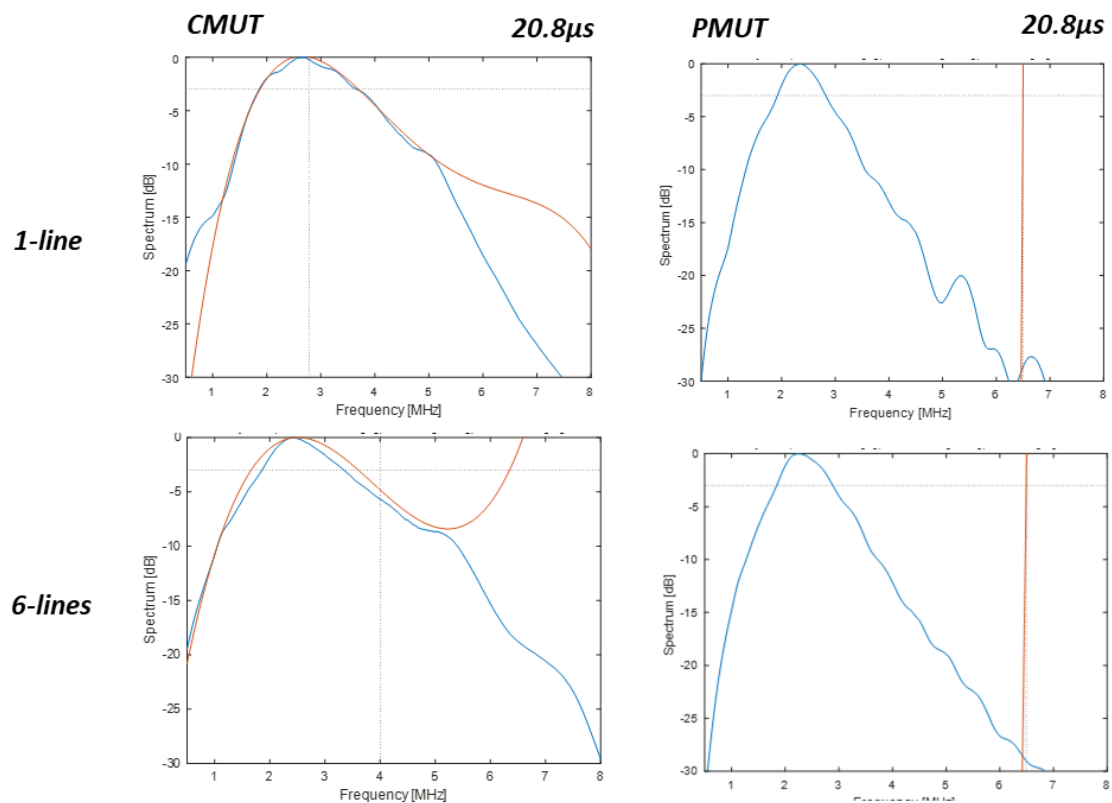
Figure 37: Impulse response spectra for 1-line and 6-lines for CMUT (left) and PMUT (right). The location of the reflector is in far field (20.8 µs). The blue lines are the measured spectra (orange lines are not optimized/inconsistent fits).

The main results derived from the spectra are (relative BW are -6dB values):
- CMUT:
  - 1-line
    - F_c: 2.90MHz
    - Relative BW: 90%
  - 6-lines
    - F_c: 2.80MHz

- • Relative BW: 95%
- • PMUT:
  - – 1-line
    - • F_c: 2.43MHz
    - • Relative BW: 63%
  - – 6-lines
    - • F_c: 2.43MHz
    - • Relative BW: 71%

The relative bandwidth for CMUT is larger than for PMUT. This is in line with expectations and earlier benchmark results [10]. In Figure 38, results for F_c and BW are shown for CMUT and PMUT, as function of time. The time is related to the distance of the reflector given the speed of sound in water (1500m/s). The CMUT devices show more variation in mainly F_c for ganged device as function of time. The CMUT also shows higher values for both F_c and BW. The higher F_c might be related to diffraction effects, for which the measurements are not compensated.

Figure 38: Centre frequency (left) and bandwidth (right) for both CMUT and PMUT with 1-line (single) and 6-lines (ganged), as function of time.

5.1.3 Transmit impulse response

The same measurements as done for pulse-echo were repeated with a hydrophone instead of a metal reflector. The distance of the hydrophone was put as close as possible to the surface of the device (NF). The impulse response measurement was performed with a unipolar single 20 ns pulse at NF. The pulse is always additive to the applied DC voltage. A typical example for NF is shown in Figure 39. The ce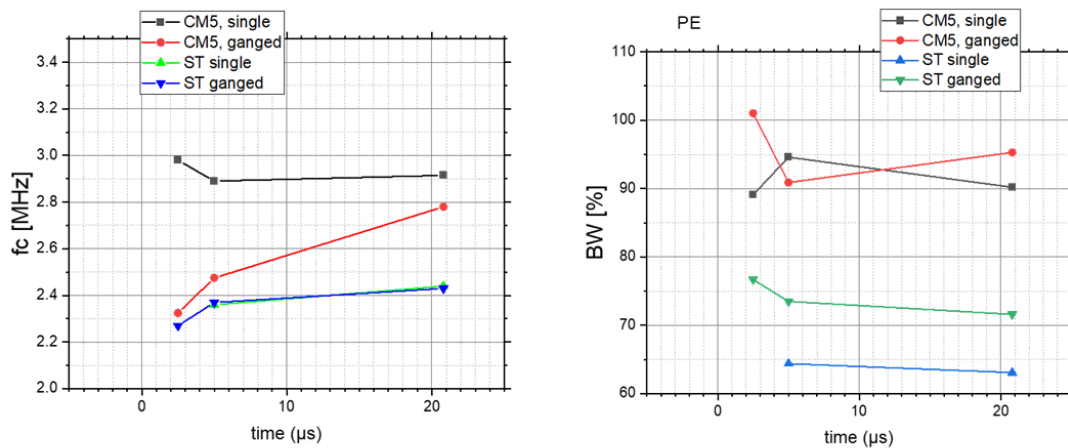ntre frequency is calculated as the middle between both -3dB points in the spectrum. The F_c for CMUT is higher than for PMUT. The absolute bandwidth for CMUT (~4MHz) is larger than for PMUT (~2MHz). The relative BW is comparable for both, due to the higher F_c used to calculate the relative BW.

The main results derived from the spectra are (relative BW are -3dB values):
- • CMUT:
  - – 1-line
    - • F_c: 4.08MHz
    - • Relative BW: 98%
    - • Absolute BW: ~4MHz
  - – 6-lines
    - • F_c: 3.17MHz

- • Relative BW: 116%
- • PMUT:
  - – 1-line
    - • F_c: 2.52MHz
    - • Relative BW: 93%
    - • Absolute BW: ~2MHz
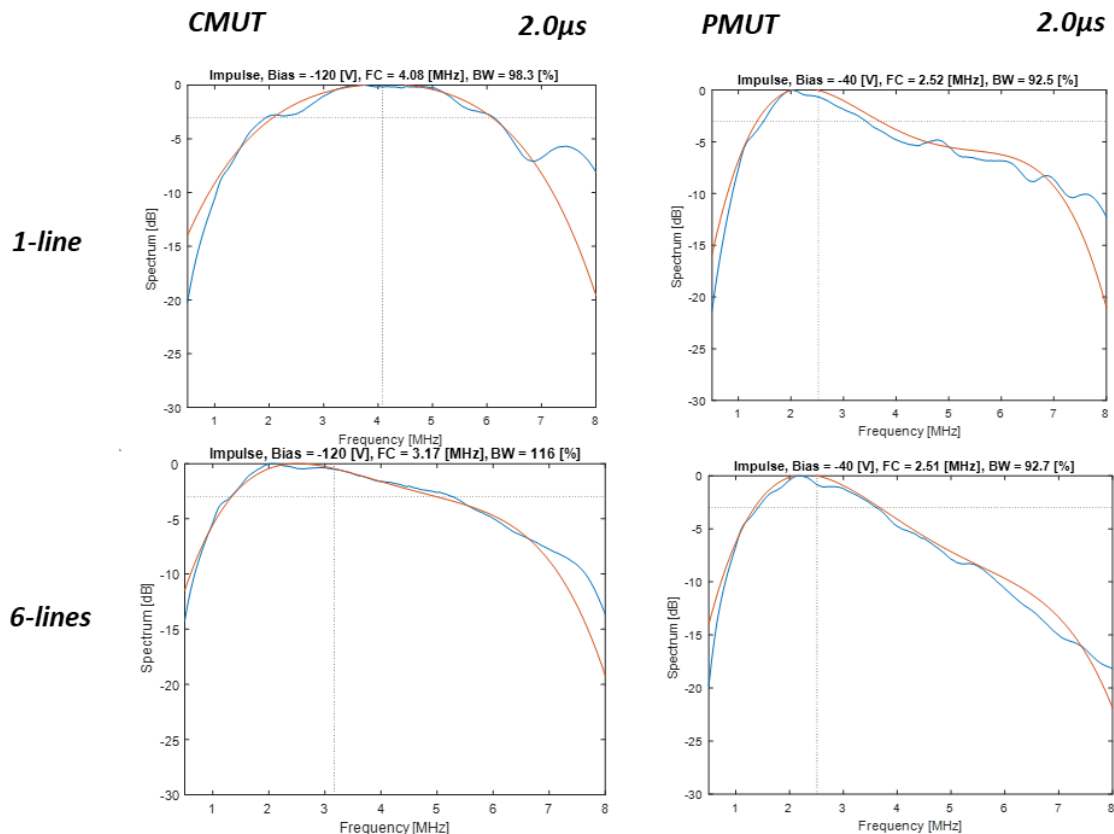 - – 6-lines
    - • F_c: 2.51MHz
    - • Relative BW: 93%

Figure 39: impulse response spectra for 1-line and 6-lines for CMUT (left) and PMUT (right). The location of the hydrophone is in near field (2.0µs). The blue lines are the measured spectra (orange lines are not optimized/inconsistent fits).

5.1.4 Transmit performance

The transmit performance was characterized with a linearity measurement: 2-cycles bipolar block wave at the centre frequency F_c of the device. The RF voltage is increased step by step to the maximally allowed peak-peak voltage. This measurement is done at NF and FF. The transmit pulse generated by the electronics ('POSITION board') and measured by hydrophone is shown in Figure 40. The generated pulse shape is more deformed for PMUT, especially for the 6-lines ganged. The reason is the higher capacitance of the PMUT devices. The single line capacitance of PMUT is ~4.8nF and ~225pF for CMUT, resulting in more deformation for PMUT. The pulse shapes measured with hydrophone in NF are good for both types without much ringing effects.
The linearity measurements (Figure 41) show better transmit performance for PMUT. The maximum pressure at 50V RF_{pp} is ~50% higher for PMUT and the pressure

Moore4Medical

Enabling "Moore for Medical"

WP4 D4.3, version 1.0
Moore4Medical
Ecsel-2019-1-876190
Page 39 of 44

sensitivity is ~50-60% higher. This is in line with expectations and earlier benchmark results, where PMUT shows better transmit performance than CMUT [10].
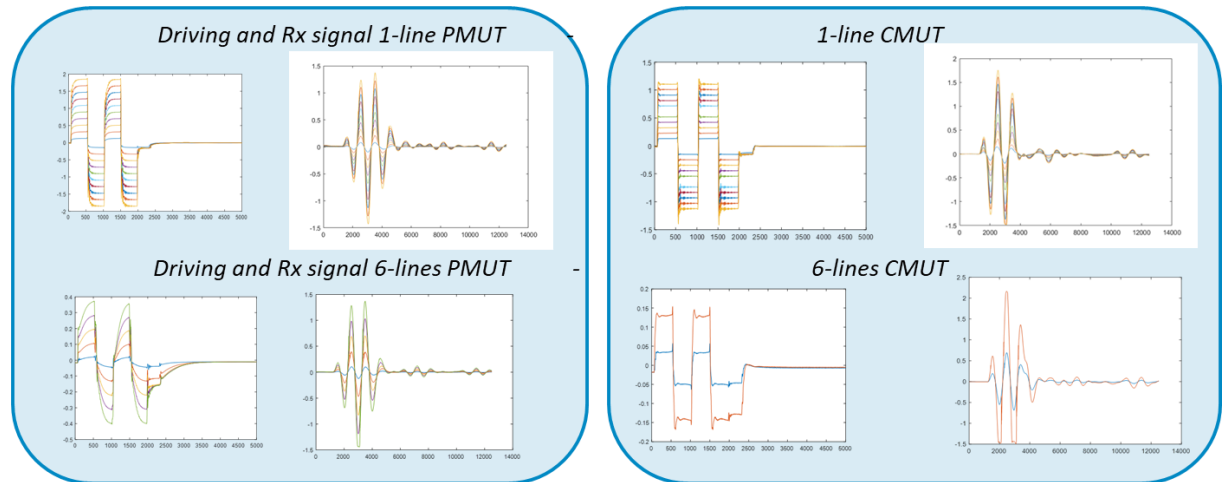

Figure 40: Pulse shape of both excitation (left graphs) and measured with hydrophone (right graphs) for PMUT (left) and CMUT (right)

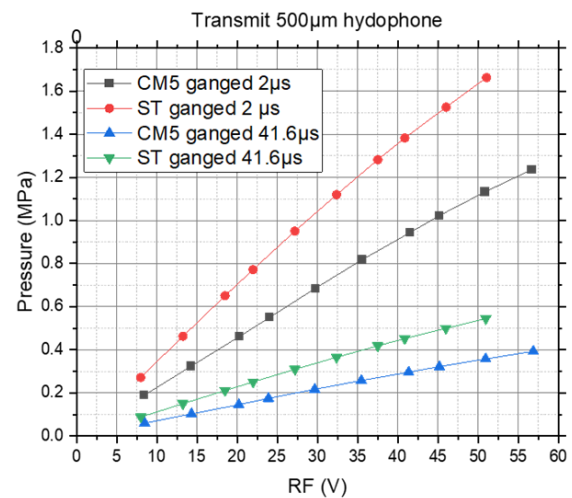|	Pressure [MPa] @ 50V RF pp	Tx sensitivity [MPa/100V]
ST 2µs	1.63	3.5
CM5 2 µs	1.11	2.28
ST 41.6µs	0.54	1.14
CM5 41.6µs	0.35	0.685

Figure 41: Linearity measurement showing sound pressure as function of peak-peak (pp) RF voltage for 6-lines (ganged) for NF and FF. The maximum pressure (@50V RF pp) and Tx sensitivity is shown in the table.

5.1.5 Pulse echo performance

The acoustic pulse echo measurements were done with a metal reflector at a far-field (FF) distance. The PE performance was characterized with a linearity measurement: 2-cycles bipolar block wave at the centre frequency F_c of the device. The RF voltage is increased step by step to the maximally allowed peak-peak voltage. The linearity measurements (Figure 42) show higher PE performance for CMUT. This is due to the higher receive sensitivity for CMUT. As shown in Chapter 5.1.4, the transmit performance is better for PMUT (~1.5x). The receive sensitivity Rx is better for CMUT, ~10x (-20.6dB) measured at Philips and ~9x (-18.9dB) measured at Roma Tre. Again, the higher receive sensitivity was expected and in line with earlier benchmark results with higher receive sensitivity for CMUT [10].

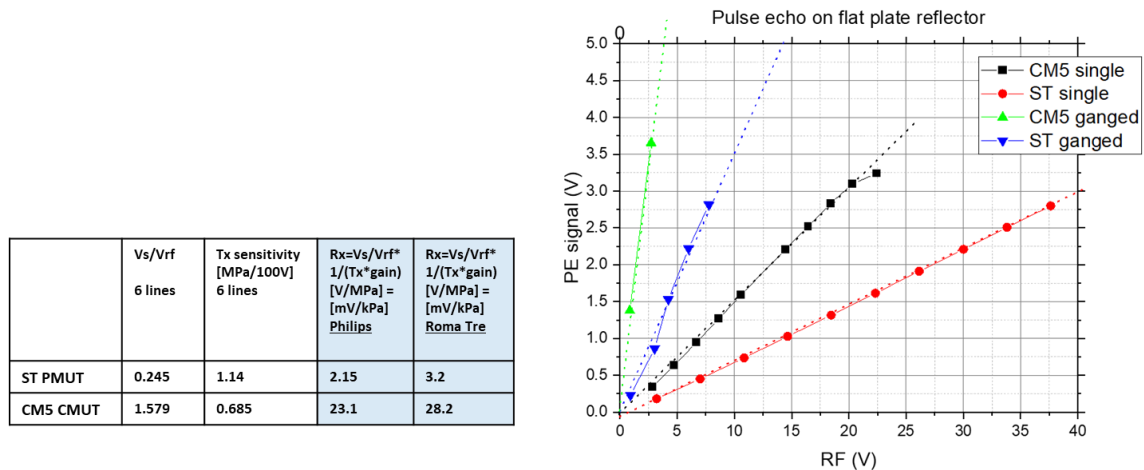|	Vs/Vrf 6 lines	Tx sensitivity [MPa/100V] 6 lines	Rx=Vs/Vrf* 1/(Tx*gain) [V/MPa] = [mV/kPa] Philips	Rx=Vs/Vrf* 1/(Tx*gain) [V/MPa] = [mV/kPa] Roma Tre
ST PMUT	0.245	1.14	2.15	3.2
CM5 CMUT	1.579	0.685	23.1	28.2

Figure 42: Linearity measurement showing sound pressure as function of peak-peak (pp) RF voltage for 1-line (single) and 6-lines (ganged) for FF. The Rx and Tx sensitivity and its ratio is shown in the table.

5.1.6 Angular acceptance

Angular acceptance measurements were performed to investigate the directionality of the generated beams for both PMUT and CMUT. In Figure 43, the results are shown for PMUT and CMUT, resulting in comparable values at -3dB (~70°).
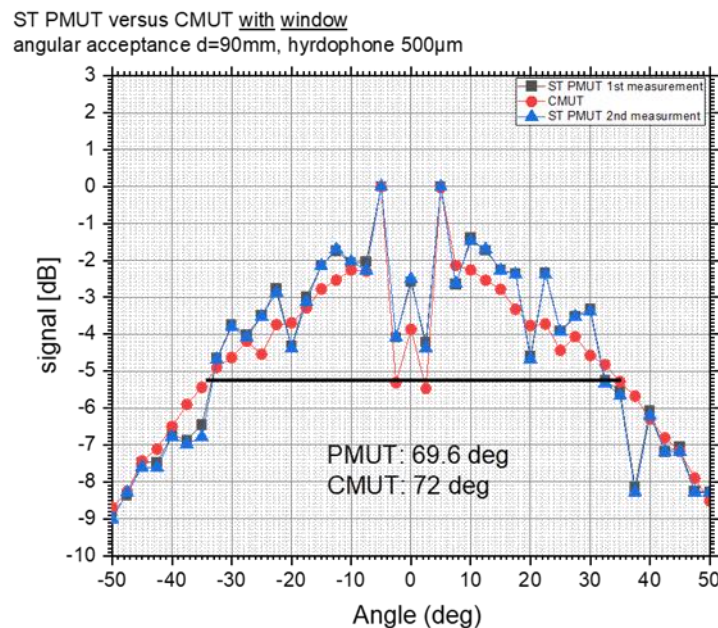

Figure 43: Angular acceptance measurements for PMUT and CMUT resulting in comparable results (~70°)

The settings used in angular acceptance measurement:
- Single line excited using RF amplifier
- Hydrophone needle Precision Acoustics SN2762 (500µm),
- Distance 60.7µsec = 90 mm,
- Rotation of hydrophone: -50 till 50° in 2.5° steps

Moore4Medical

Enabling "Moore for Medical"

WP4 D4.3, version 1.0
Moore4Medical
Ecsel-2019-1-876190
Page 41 of 44

- Excitation with 5 sine pulse, f=2.6MHz;
- Bias -40V for PMUT/ -120V for CMUT

5.2 Benchmark results measured at Roma Tre University

Experimental benchmarking of both PMUT and CMUT 1-D arrays has been carried out. Both arrays were packaged and characterized using the procedures and experimental setups described in Section 4.

5.2.1 Electro-mechanical parameters

The main electro-mechanical parameters reported in Table 7 have been extracted from impedance spectroscopy measurements carried out on all the 64 array elements of the arrays in air-coupled conditions. The bias voltages applied to the PMUT and CMUT arrays are 40 V and 120 V, respectively. The table reports the values of the mean element capacitance C_p and the resonance frequency F_r, and their relative standard deviation (RSD), as well as the electromechanical coupling factor k_T^2 and the parasitic series resistance R_s.

Table 7: Electro-mechanical parameters

	PMUT	CMUT
Bias voltage	40 V	120 V
C_p (%RSD)	2.14 nF (0.87 %)	91.7 pF (0.42 %)
F_r (%RSD)	3.09 MHz (0.59 %)	3.3 MHz (0.58 %)
k_T^2	0.08	0.3
R_s	11.5 Ω	30 Ω

The bias voltage that allows optimized operation is noticeably higher in the CMUT case (3x), which may be a disadvantage related to patient safety. On the other hand, the PMUT suffers from a higher capacitance (~20x), due to the high dielectric constant of PZT, with a negative impact on the electromechanical coupling factor and, consequently, on the efficiency and noise performance.

5.2.2 Small signal electro-acoustic performance

Small signal electro-acoustic performance has been benchmarked by processing the results of hydrophone and pulse-echo measurements carried out in water-coupled conditions using low-voltage, broadband excitation signals. The assessed parameters, shown in Table 8, are the TX and RX peak sensitivities, and the two-way (TW) centre frequency and fractional bandwidth.

Table 8: Small signal electro-acoustic parameters

	PMUT	CMUT
TX pk. Sensitivity	31 kPa/V	14.1 kPa/V
RX pk. Sensitivity	3.2 mV/kPa	28.2 mV/kPa
TW centre frequency (-6dB % BW)	2.5 MHz (83 %)	2.5 MHz (120 %)

The TX sensitivity is higher for the PMUT (~2x), while the RX sensitivity is higher for the CMUT (~3x). Fractional bandwidth of the CMUT is higher than the PMUT (~1.5x).

5.2.3 Large signal electro-acoustic performance

Large signal electro-acoustic performance has been benchmarked by processing the results of hydrophone measurements carried out in water-coupled conditions using high voltage, narrowband excitation signals. The assessed parameters, shown in Table 9, are the maximum peak-to-peak pressure at the transducer surface, and the second harmonic-to-fundamental-ratio (HFR) computed at the maximum pressure achievable and at the typical pressure required for harmonic imaging applications (i.e., 1 MPa).

Table 9: Large signal electro-acoustic parameters

	PMUT	CMUT
Maximum pk-pk pressure	1.8 MPa ($40\ V_{ac}$)	1.4 MPa ($50\ V_{ac}$)
HFR @ max pressure	-22 dB	-10 dB
HFR @ 1 MPa	-29 dB	-14 dB

The maximum peak-to-peak pressure achievable with the PMUT is higher, and both CMUT and PMUT are capable of generating the pressure of 1 MPa$_{pk-pk}$ required for harmonic imaging applications. Noticeably, the PMUT is capable of generating such a pressure with a -29dB second harmonic level that makes it suitable for harmonic imaging.

5.3 Conclusions

After first benchmark experiments carried out at Roma Tre University, comparable measurements were done at Philips for both devices. The main conclusion is that measurement results on both sites are in line with each other. Other conclusions are:

- CMUT
  - Larger round-trip sensitivity → factor ~6x better than PMUT
  - Larger band width → important for image resolution
- PMUT
  - Larger transmit sensitivity → factor ~1.5-2x better than CMUT
  - Lower harmonic distortion → factor ~2x → important for 2nd harmonic imaging
- Differences between CMUT and PMUT are in line with earlier benchmark results EU project Position

6 References

1. HTTPS://CRITICALCARENORTHAMPTON.COM/2019/04/15/THE-FINAL-BATTLE-PORTABLE-ULTRASOUND-DEVICES/#MORE-21570
2. HTTPS://WWW.EXO.INC/EXO-WORKS/
3. HTTPS://WWW.BUTTERFLYNETWORK.COM/
4. A.S. SAVOIA (ROMA TRE UNIVERSITY), PRIVATE COMMUNICATION
5. ROB VAN SCHAIJK, CMUT: A VERSATILE ULTRASONIC PLATFORM DEVELOPED BY PHILIPS, MEMS SEMINAR 2019
6. C. VAN HEESCH ET AL., "COLLAPSE -MODE CMUT: DESIGN AND CHARACTERIZATION," INVITED PRESENTATION AT THE IEEE INTERNATIONAL ULTRASONICS SYMPOSIUM (IUS) 2018, 22-25 OCTOBER 2018, KOBE JAPAN. HTTP://SITES.IEEE.ORG/IUS-2018/
7. http://position-2.eu/
8. http://ulimpia-project.eu/
9. http://informed-project.eu/downloads/F2R.pdf
10. https://www.s2e2.fr/wp-content/uploads/2022/03/CMUT-PMUT-Benchmark-Technical-Whitepaper.pdf
11. REPORT BY SYSTEM PLUS CONSULTING 'BUTTERFLY NETWORK IQ CMUT DIE' 2020
12. E. BONI ET AL. , "ULA-OP 256: A 256-CHANNEL OPEN SCANNER FOR DEVELOPMENT AND REAL-TIME IMPLEMENTATION OF NEW ULTRASOUND METHODS," IEEE TRANS. ULTRASON., FERROELECT., FREQ. CONTR. 2016.

Moore4Medical

Enabling "Moore for Medical"

7 Abbreviations

Abbreviations	Meaning
AC	Alternating current
ASIC	Application-specific integrated circuit
BW	Bandwidth
CMOS	Complementary metal oxide semiconductor
DC	Direct current
DoE	Design of Experiments
EM	Electromechanical
HF	High frequency
CMUT	Capacitive micromachined ultrasonic transducer
DRIE	Deep reactive-ion etching
Fc	Centre Frequency
FEM	Finite Element Modelling
FF	Far field
HV	High voltage
ICE	Intracardiac echocardiography
IVUS	Intravascular ultrasound
LF	Low frequency
MEMS	Micro-electromechanical systems
MUT	Micromachined ultrasonic transducer
NF	Near field
Pb	Lead
PBR	Polybutadiene
PMUT	Piezoelectric micromachined ultrasonic transducer
P_{pk}	Process capability
PZT	Lead zirconate titanate
RH	Relative Humidity
RF	Radio frequency
RX	Receive
Si	Silicon
SOI	Silicon-on-Isolator
TEE	Transesophageal echocardiography
TPX	Polymethyl pentene, it is commonly called TPX, which is a trademark of Mitsui Chemicals
TSV	Through-Silicon Via
TX	Transmit
ULV	Ultra-low Voltage
US	Ultrasound
VC	Collapse Voltage